

# Deconstructing the Crystal Structures of Metal–Organic Frameworks and Related Materials into Their Underlying Nets

Michael O’Keeffe<sup>\*,†,‡</sup> and Omar M. Yaghi<sup>\*,‡,§</sup>

<sup>†</sup>Department of Chemistry and Biochemistry, Arizona State University, Tempe, Arizona 85287, United States

<sup>‡</sup>Center for Reticular Chemistry, Center for Global Mentoring, Department of Chemistry and Biochemistry, University of California—Los Angeles, 607 Charles E. Young Dr. East, Los Angeles, California 90095, United States

<sup>§</sup>Graduate School of EEWS, Korea Advanced Institute of Science and Technology, Daejeon, Korea

## CONTENTS

|   |     |
|---|-----|
| 1. Introduction   | 675 |
| 2. Identification, Description, and Characterization of Nets      | 676 |
| 3. Edge Nets, Augmented Nets, and the Underlying Topology         | 677 |
| 4. The Deconstruction of Crystal Structures                       | 678 |
| 4.1. Crystals with Corundum Net (cor)                             | 678 |
| 4.2. Some Symmetrical Metal-Containing SBUs                       | 679 |
| 4.3. Some Simple Organic SBUs                                     | 680 |
| 4.4. Some Structures with the pts Topology                        | 683 |
| 4.5. Two MOFs Whose Preferred Description Is Not the pts Topology | 684 |
| 4.6. MOFs with Multiple Links between SBUs                        | 685 |
| 4.7. Examples of Lower-Symmetry Metal-Containing SBUs             | 686 |
| 5. Some Case Studies  | 687 |
| 5.1. A MOF with ubt Topology                                      | 687 |
| 5.2. MOFs with Hexatopic Carboxylate Linkers                      | 687 |
| 5.3. MOFs with Octatopic Linkers                                  | 689 |
| 5.4. More on Metal Cluster SBUs                                   | 690 |
| 5.5. More Structures with Linked MOPs                             | 691 |
| 5.6. A Cyclodextrin MOF   | 694 |
| 5.7. The Hierarchical Underlying Nets of MIL-101 and MIL-100      | 694 |
| 6. MOFs with Rod SBUs   | 696 |
| 6.1. SBUs as Zigzag Ladders                                       | 696 |
| 6.2. A MOF with a Twisted Ladder Rod SBU                          | 697 |
| 6.3. A MOF with Rod SBUs of Linked Tetrahedra                     | 697 |
| 6.4. Two-Way Rod SBUs of Linked Tetrahedra                        | 697 |
| 6.5. MOFs with Rod SBUs of Linked Octahedra                       | 698 |
| 6.6. Rod SBUs That Resist Simplification                          | 698 |
| 7. MOFs with Ring SBUs  | 698 |
| 7.1. Coda   | 699 |
| 8. Concluding Remarks   | 699 |
| Author Information  | 699 |
| Biographies   | 699 |
| Acknowledgment  | 700 |
| References  | 700 |

## 1. INTRODUCTION

The synthesis and characterization of metal–organic frameworks (MOFs) is one of the most rapidly developing areas of chemical science. These materials have unquestionably enormous potential for many practical applications, as detailed elsewhere in this issue, but they also often have exceptionally beautiful structures. It is the identification and description of the *nets* that describe the *underlying topology* of these structures that is the main topic of this review. In particular we emphasize that this is *not* a review of MOF structures per se.

Why should we care about nets and related structural aspects of crystals? First and foremost, as chemists we recognize that the very core of our science lies in describing, and perhaps understanding, how atoms organize themselves, sometimes with our help, in chemical compounds. Such knowledge is also essential to designed (“rational”) synthesis of MOFs and related materials from component parts, as has been stressed recently.<sup>1</sup> For this, of course, one needs to know the principal possibilities, which, as discussed below, have been established systematically only in the past few years. By *deconstruction*, we mean simply the reverse of the thought process that goes into designed synthesis, that is, breaking down a complex structure into its fundamental units without losing their chemical significance. One can think of it as reverse engineering.

Another reason for knowing about nets and their occurrences is a result of the dramatic advances in methods of computer simulation of MOF–adsorbate interactions, especially calculated adsorption isotherms, which makes the computer prescreening of potential materials an attractive procedure.<sup>2</sup> Of course, to do this usefully it must be performed for materials for which there is a reasonable prospect of actual synthesis, which in turn will be done by design.

From the very earliest days of crystallography, simple inorganic structures were shown as “ball-and-stick” models in which the balls were the atoms and the sticks corresponded to bonds presumed to exist between nearest-neighbor atoms.<sup>3</sup> It was early realized, particularly by Wells,<sup>4</sup> that such models could be considered as representations or *embeddings* of special kinds of abstract graphs called *nets* (defined below) with the vertices of the graph corresponding to the atoms and the edges (links) of the

**Special Issue:** 2012 Metal–Organic Frameworks

**Received:** June 6, 2011

**Published:** September 15, 2011

graph corresponding to the bonds. Wells devoted much effort to enumerating nets, but he focused almost entirely on structures with three- and/or four-coordinated vertices and placed special emphasis on structures with shortest cycles (closed paths around the net) of all the same size; he called these structures *uniform* nets. Although he correctly recognized the importance of structures with symmetry-related vertices and edges, in fact, he found only very few of those now known.

It also became apparent that the same topology (net) was found in many different chemical contexts. It was also realized that the edges and vertices of the net could be respectively polyatomic linkers and clusters. The work of the Iwamoto group on cyanides is notable in this respect. Complex cyanides with nets of forms of silica (cristobalite, tridymite and keatite) of other binary compounds such as rutile (TiO<sub>2</sub>), pyrite (FeS<sub>2</sub>), and cooperite (PtS) were prepared and their nets identified.<sup>5</sup> The term “mineralomimetic” was coined to describe this kind of chemistry.

An important next step was the realization that, in fact, certain topologies could be targeted, especially for cyanides, by assembling appropriately shaped components.<sup>6,7</sup> The wide variety of chemical compounds amenable to this approach was subsequently emphasized in several reviews.<sup>7,8</sup> It should be emphasized, however, that it was in general rare for an underlying net to be identified in the older literature, and furthermore, when a net was identified, it was often done incorrectly. This last criticism applies far too often also to recent work. Indeed, the diligent reader will find that some of the examples adduced in this review were originally assigned either to no topology or to an incorrect one. However, it is less the purpose here to correct errors than to point the way to better analyses in the future.

The discovery of MOFs, a term used here particularly to describe *robust and highly porous* metal–organic frameworks, led to the recognition that, in order to truly obtain structures by design, one had first to identify the principal topological possibilities for nets. These, which were termed *default structures*,<sup>9,10</sup> were identified as those with high point symmetry at the vertices and with a small number of different kinds of vertex and edge—two conditions that are, of course, highly correlated. Subsequent analysis of published structures confirmed the predominance of these default topologies.<sup>11</sup>

The discipline of preparing materials of targeted geometry by design is termed *reticular chemistry*<sup>10</sup> and a series of compounds with the same underlying topology (net) is called an *isorecticular series*.<sup>12</sup> As already mentioned, for successful reticular chemistry one needs to know the principal topologies, and a concerted effort was made to enumerate them.<sup>13</sup> The most important of these are nets with one kind of edge (*edge transitive*) most of which were unknown prior to this work but are now realized to be of special importance. A review under the rubric “Taxonomy of Nets and the Design of Materials” has been published.<sup>14</sup>

Data for many of the nets most important for reticular chemistry are collected in a searchable database known as the Reticular Chemistry Structure Resource (RCSR).<sup>15</sup> There nets are assigned three-letter symbols such as **abc**, or symbols with extensions as in **abc-d** (see below). This database is rather small (about 2000 entries). A much larger database is being developed in the EPINET project, which currently contains about 15 000 three-periodic nets.<sup>16</sup> The computer program TOPOS recognizes even more, about 70 000.<sup>17</sup> In this connection, mention should also be made to the extensive enumerations of sphere packings by Fischer and associates.<sup>18</sup> The nets of these structures

have just one kind of vertex and have an embedding in which all the shortest (and equal) intervertex distances correspond to edges of the net. Most of these are incorporated in the RCSR.

## 2. IDENTIFICATION, DESCRIPTION, AND CHARACTERIZATION OF NETS

A net is just a special sort of graph. It is *simple*, meaning that there is at most one undirected edge that links any pair of vertices, and there are no loops (edges linking a vertex to itself). A net is also *connected*, meaning that every vertex is linked to every other by a continuous path of edges. The net of a polyhedron is finite. In crystals we will have infinite nets that are one-, two-, or three-periodic (“dimensional”). The emphasis here will be on three-periodic nets. Graph-theoretical aspects, in particular terminology and definitions, have been given elsewhere.<sup>19</sup>

By “underlying topology” we mean the innate structure of the net associated with the crystal structure. Topology is really a branch of mathematics (or several branches as some would have it). However, here we use the term, following common usage, to refer to the combinatorial structure of a graph that is invariant in different embeddings.<sup>20</sup>

In this review we show how a net is extracted from a crystal structure. The first question is, what is the identity of the net? This can be answered in a meaningful way only by saying that it is identical to a previously known net that has an identifier (such as a RCSR symbol). Otherwise, the net is new. The only algorithm devised to do this in a mathematically rigorous way is realized in Olaf Delgado–Friedrichs’ program Systre.<sup>21</sup> It should be mentioned, though, that in practice the program TOPOS<sup>17</sup> also solves this problem with a high degree of certainty.

The second question to ask of the net is, what is the symmetry? By this we mean the combinatorial symmetry which, for the nets discussed here, is isomorphic with a space group and is the maximum possible symmetry of an embedding. As far as we know only Systre<sup>21</sup> answers this question. As a bonus, Systre computes an embedding (a realization with space group, unit cell parameters, vertex coordinates, and edge specification) in that symmetry. Occasionally, in practice very rarely, one encounters nets that have nonrigid body symmetries; we give an example below (section 5.2). Such nets are not currently considered by Systre.

The local topology of a vertex in a net is sometimes characterized by a point symbol or a vertex symbol. The point symbol, introduced by Wells,<sup>4</sup> gives information about the shortest cycles at each angle of a vertex. The point symbol is of the form  $A^a.B^b\dots$  and signifies that there are  $a$  angles at which the shortest cycle is an  $A$ -cycle,  $b$  angles at which the shortest cycle is a  $B$ -cycle, etc. By convention  $A < B < \dots$  and  $a + b + \dots = z(z - 1)/2$ , where  $z$  is the coordination number of the vertex and  $z(z - 1)/2$  is the number of angles at that vertex. Point symbols for nets are conveniently obtained from TOPOS.

Our preference is for *vertex symbols* (also given by TOPOS), which give information about the number of rings (cycles that are not the sum of two shorter cycles) at each angle in a vertex.<sup>22</sup> However, these become cumbersome for vertices of higher than six-coordination. These symbols are used to characterize the nets in the RCSR and in the *Atlas of Zeolite Framework Types*.<sup>23</sup>

Nets with one kind of vertex (i.e., those for which all the vertices are related by symmetry operations in their most symmetrical embeddings) are often called *uninodal*, those with two kinds of vertex *binodal*, etc.

There are two common practices that we would like to discourage. The first is that of calling a point symbol a “Schläfli symbol”. In universally accepted mathematical usage the latter is a symbol for a regular tiling. In three-dimensional Euclidean space, there is only one such tiling—a face-to-face tiling by cubes for which the Schläfli symbol is  $\{4,3,4\}$  (the point symbol for the net is  $4^{12}.6^3$ ). The distinction between various symbols for vertex configurations and tilings has been discussed fully recently.<sup>24</sup> In older papers, vertex symbols were also incorrectly called Schläfli symbols.<sup>22</sup>

The second usage we would like to discourage is that of referring to a point symbol or a vertex symbol as a “topology”. It is not; many nets with different topologies have vertices with the same point symbol. For example, the RCSR contains 14 distinct uninodal nets with point symbol  $6^6$ , and if one includes polytypes of the diamond/lonsdaleite type, there is an infinite number of nets in which all vertices have point symbol  $6^6$ . By far the best way of specifying a net, particularly a new, or previously undocumented, one is by a Systre-readable file. TOPOS can export Systre-readable files. For nets in the RCSR database, the RCSR symbol should be an adequate identifier.

Recent advances in our knowledge of three-periodic nets have come from tiling theory. In a tiling, space is divided into generalized polyhedra (*cages*) sharing faces (a “face-to-face” tiling). In a *natural* tiling, the tiling has the same symmetry as the intrinsic symmetry of the net, and no one face of a tile is bigger (has more edges) than the rest. Subject to these constraints, the natural tiling consists of the smallest possible tiles.<sup>13a</sup> For some low symmetry nets, additional rules may be needed to obtain a unique tiling for a net.<sup>25</sup> A *simple polyhedron* is one in which exactly three edges meet at each vertex. A *simple tiling* is a tiling by simple polyhedra in which exactly four tiles meet at a vertex and exactly three meet at an edge. Foams and cellular materials are simple tilings.

A convenient measure of “regularity” of a net is the *transitivity*, a set of four integers  $pqrs$  that states that a tiling has  $p$  kinds of vertex,  $q$  kinds of edge,  $r$  kinds of face, and  $s$  kinds of tile. The five regular nets<sup>13a</sup> are the only ones with a natural tiling with transitivity 1111. Edge-transitive nets have transitivity  $p1rs$  with  $p = 1$  or 2.

It is common in chemistry to refer to nets in which  $k$  edges meet at every vertex as  $k$ -connected. However, in graph theory  $k$ -connectivity has a quite different meaning,<sup>19</sup> so we prefer to use  $k$ -coordinated or  $k$ -c for short. Nets with vertices with two or more different coordinations are written as  $(k_1, k_2, \dots)$ -c.

For linkers with respectively two, three, four, five, six, ... coordinating groups, we use the accepted terminology of ditopic, tritopic, tetratopic, pentatopic, hexatopic, ...

This review discusses how one goes about abstracting the underlying topology from an experimental crystal structure of materials like MOFs. It is hoped that this will complement a recent article in which an analysis of the structures of the more than 6000 such materials in the Cambridge Structural Database was undertaken in an automated manner using TOPOS.<sup>26</sup> Clearly only a few illustrative examples of those 6000 structures can be presented here. These have been chosen to illustrate general principals, to point up occasions where there may be no clear choice of a unique underlying topology, and also to illustrate some minor differences of opinion on how best to deconstruct crystal structures.

Readers interested in the variety of known three-periodic nets are referred to a recent comprehensive review.<sup>27</sup> For the deconstruction of zero-periodic metal–organic polyhedra and descriptions

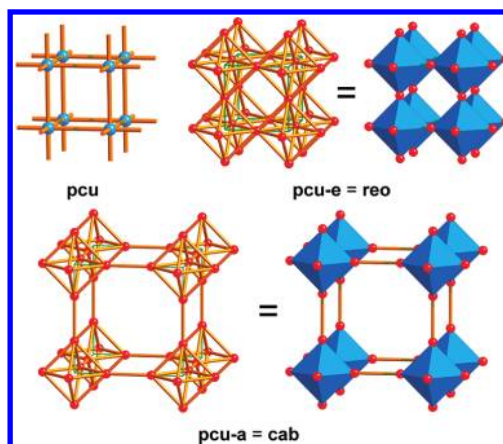


Figure 1. Nets derived from the net of the primitive cubic lattice (**pcu**).

of their underlying topology, reference is also made to a recent review.<sup>28</sup>

### 3. EDGE NETS, AUGMENTED NETS, AND THE UNDERLYING TOPOLOGY

In Figure 1 the net (RCSR symbol **pcu**) of the primitive cubic lattice is shown. Also shown is the *edge net*, in which new vertices are placed in the middle of each original edge and vertices in edges with a common original vertex are joined together to form an octahedron around the original vertex. One can also think of the new net as an *expansion* of the original net.<sup>9</sup> In any event, the new net is symbolized **pcu-e**. In this case the net is simple and “important” enough to merit its own RCSR symbol, which is **reo** (the O net in  $\text{ReO}_3$  has this structure). Note that the new net is not an *edge graph* in the mathematical sense, as in that case the new vertices would form a complete graph around the original vertex (thus including in this case edges linking opposite corners of the octahedron).<sup>29</sup>

Zeolite frameworks have stoichiometry  $\text{TX}_2$ . Here T is a tetrahedrally coordinated atom and the X atoms form a net of corner-sharing tetrahedra. In characterizing zeolite topology, the net is considered as four-coordinated with T atoms at the vertices and  $-X-$  as the edges. Thus, for faujasite with zeolite framework type<sup>23</sup> **FAU** (RCSR symbol **fau**), the framework is said to have the 4-c **fau** topology. If we want to explicitly describe the net of X atoms we use the 6-c net **fau-e**. The important point is that we consider the expanded and unexpanded structures to have the same underlying net (“underlying topology”).

Figure 1 also shows an *augmented net* derived from **pcu**. Now the vertices of the original net are replaced by their vertex figures—polyhedron or polygon—in this instance an octahedron. The symbol for the new net is **pcu-a**. Again in this case there is an alternative symbol—**cab**—reflecting the fact that the net is the net of the B atoms in  $\text{CaB}_6$ . For finite polyhedra the process of augmentation has long been termed *truncation*, but clearly the process of truncation (amputation of part of a polyhedron containing that vertex) cannot be carried out for two- or three-periodic nets.

The process of augmentation, like that of forming edge nets, is not based on graph theoretical foundation as again, in general, the new sets of vertices and edges do not form complete graphs. In fact, the new net derives essentially from a symmetric embedding of the original net. This is illustrated in Figure 2 for

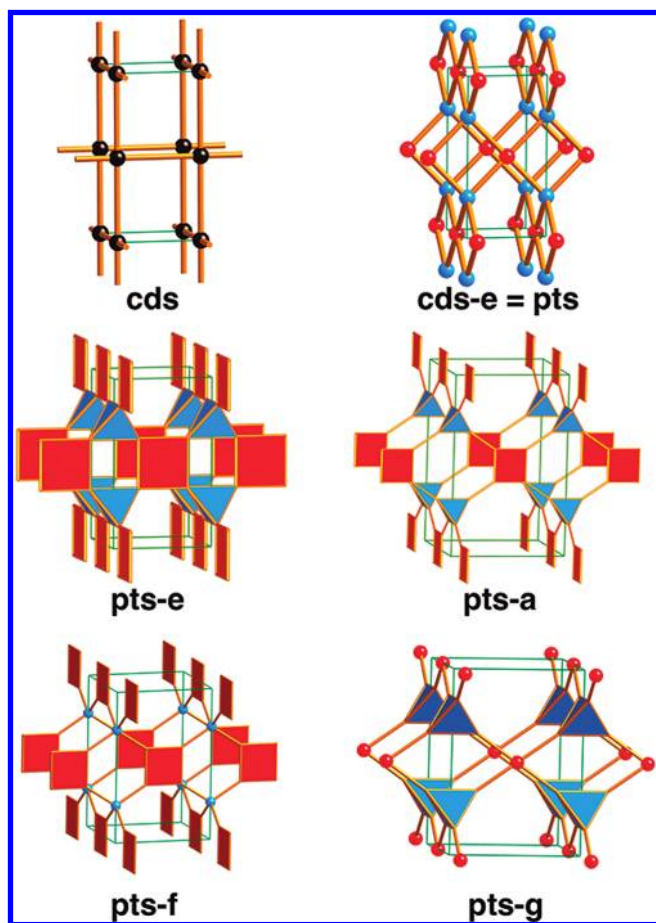


Figure 2. Nets related to the PtS (cooperite) net (*pts*).

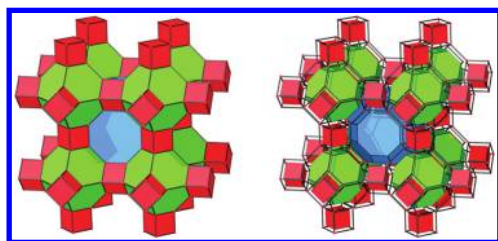


Figure 3. The net (*lta*) of the zeolite with framework type LTA. It should be clear from Figure 1 that this net could be assigned RCSR symbol *reo-e*. On the right the tiles of the structure are slightly shrunk to make the tiling clearer.

the pair *pts*, *pts-a* in a maximum-symmetry embedding. Notice that the two four-coordinated vertices are treated differently; in particular, the one with four coplanar edges lying in a mirror plane is replaced by a rectangle (square) in the augmented net.

In a net with more than one kind of vertex, there is the possibility that not all vertices are augmented. Thus, for *pts* one could leave the tetrahedral vertex but replace the square coordinated vertex by a square of vertices producing the structure identified as *pts-f* in Figure 2. Alternatively, leaving the square vertex alone and augmenting the tetrahedral vertex produces the pattern identified as *pts-g* in Figure 2. Both of these “half-augmented” nets, as well as the edge net and the augmented net, are all considered to have the same underlying *pts* topology.

We will see later (section 4.7) that we may have “augmented” nets with lower intrinsic symmetry than the parent net if the

augmented net has vertices replaced by “vertex figures” with additional or missing edges. These are considered to have the same underlying topology.

Notice that we generally avoid multiple generations of edge- or augmented-nets. Thus, the zeolite framework *lta* may be seen (Figure 3) to be *reo-a* = *pcu-e-a*. Reducing *lta* down to an underlying topology of *pcu* would eliminate vital information about the cages (tiles) of this structure. Likewise, reducing *pts* to *cde-e* (see Figure 2), although it leads to interesting insights, would obscure the basic nature of materials based on the *pts-a* structure. The drawings in Figure 3 also illustrate a tiling. In this case it is a simple tiling.

#### 4. THE DECONSTRUCTION OF CRYSTAL STRUCTURES

MOFs, by definition, are made up of two kinds of *secondary building unit* (SBU). One kind is organic linkers that, as shown below, may be ditopic or polytopic. The second kind of SBU may be a metal atom or (most commonly) a finite polyatomic cluster containing two or more metal atoms or an infinite unit such as a one-periodic rod of atoms. The two types of SBU are treated slightly differently in a way that reflects their different roles in the design and synthesis process.

Metal-containing SBUs are formed at the time of synthesis using conditions (e.g., temperature, pH) designed to produce just that SBU. Their shape is defined by *points of extension*<sup>10a</sup> where they connect to organic linking components. This shape is generally a polygon, polyhedron, or a rod that often does not reveal the full internal structure of the SBU (we give examples below).

On the other hand, organic SBUs are preformed to a custom shape. The essence of systematic MOF chemistry (reticular chemistry) is the combination of a given metal-containing SBU with a variety of organic SBUs. In particular, the latter may have the same topology but a different metric, producing, one anticipates, an *isoreticular series* of structures with the same underlying net. Because of the flexibility of design of these organic components, it is important to identify all the branching points (vertices) and individual links (edges) rather than just identifying the envelope (points of extension).

The deconstructive procedure we follow when confronted with a new MOF structure is as follows. First, the different vertices of the net are identified, as shown in the examples below. Next, the coordinates of one of each crystallographic type of vertex and those of its neighbors are presented to Systre together with the crystal symmetry. Systre will then identify the true combinatorial symmetry of the net (except for the rare cases of noncrystallographic symmetry as discussed in § 5.2). If the net is in the RCSR database, Systre will identify it. For nets new to Systre, TOPOS can be consulted for point and vertex symbols and for tiling data. Several detailed examples are given in the Supporting Information.

The crystal structure drawings in this paper are designed to illustrate the deconstruction process rather than to illustrate structures themselves. In particular, atoms irrelevant to topology, such as H, methyl groups, and monotopic coordinating groups, are usually omitted. We use the color codes C, black; O, red; N, green; and metal, blue.

##### 4.1. Crystals with Corundum Net (*cor*)

Corundum,  $\text{Al}_2\text{O}_3$ , has a simple crystal structure with one kind of octahedral Al and one kind of tetrahedral O; i.e., it has a binodal (4,6)-c net, symbol *cor*, and is commonly found as the

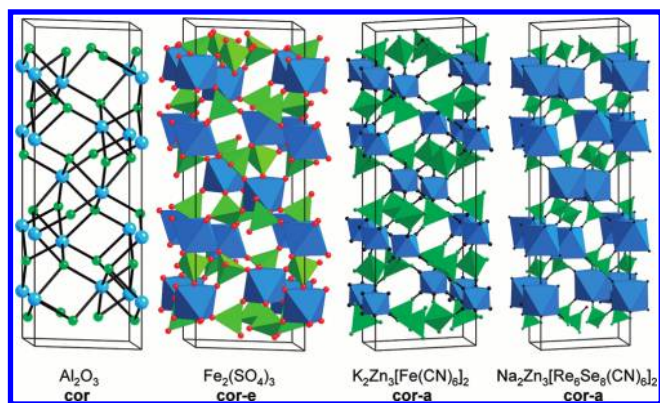


Figure 4. Examples of materials with the underlying net **cor** (corundum). See also Figure 5.

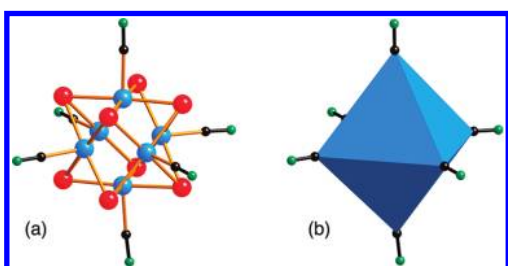


Figure 5. (a) The  $\text{Re}_6\text{Se}_8(\text{CN})_6$  unit. (b) The same abstracted as an octahedral SBU.

structure of sesquioxides, sesquisulfides, etc. The same topology is found in compounds like  $\text{Fe}_2(\text{SO}_4)_3$ , now with  $-\text{O}-$  links as edges. The O atom net is now **cor-e**. In compounds like  $\text{K}_2\text{Zn}_3[\text{Fe}(\text{CN})_6]_2 = \text{K}_2\text{Fe}_2[\text{Zn}(\text{NC})_4]_3$ , there is again the same underlying topology.<sup>30</sup> Now Fe and Zn are joined by  $-\text{C}-\text{N}-$  links to form the **cor** net, or alternatively,  $\text{ZnN}_4$  tetrahedra and  $\text{FeC}_6$  octahedra are joined in the **cor-a** net as shown in Figure 4. K ions are in cavities of the structure.

Interesting cyanide compounds based on the **cor** net were prepared more recently.<sup>31</sup> In these, the octahedral cation is replaced by an SBU with composition  $\text{Re}_6\text{Se}_8$  with CN groups attached to the Re so that the octahedral group is  $\text{Se}_8\text{Re}_6\text{C}_6$ , as shown in Figure 5. The C atoms of the SBU are the points of extension and define the (octahedral) shape of the SBU. This SBU is linked to  $\text{ZnN}_4$  tetrahedra by C–N bonds. Na ions and water molecules are in the large cavities. The increase in unit cell volume over that of the original  $\text{Al}_2\text{O}_3$  is a factor of 49. It is this dramatic change in scale that makes MOF structures intrinsically open and provides the basis for their applications in gas storage, among others.

#### 4.2. Some Symmetrical Metal-Containing SBUs

In Figure 5 it was shown how the  $\text{Se}_8\text{Re}_6\text{C}_6$  unit could be abstracted as an octahedron and ultimately as an octahedrally coordinated vertex of the **cor** net. Here some other examples of symmetrical metal-cluster SBUs are shown and similarly abstracted as regular geometrical shapes formed by their points of extension. In MOFs they are linked by organic linkers such as carboxylates. Some have been known for a long time in molecules such as copper acetate, basic zinc acetate, and basic chromium acetate; a review describing 131 of these molecular clusters has been given recently and this can be consulted for references.<sup>32</sup>

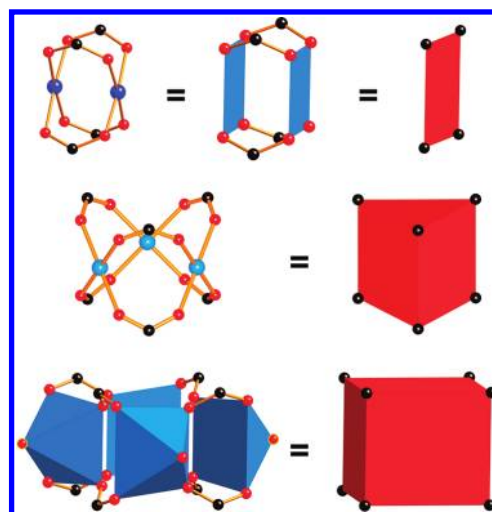


Figure 6. SBUs with two, three, or four square planar or square pyramidal units.

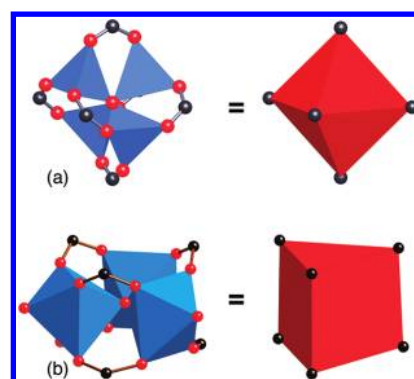


Figure 7. (a) The basic zinc acetate SBU  $\text{OZn}_4(\text{CO}_2)_6$ . (b) The basic chromium acetate SBU  $\text{OCr}_3(\text{CO}_2)_3$ .

Figure 6 shows SBUs consisting of two, three, or four square planar or square pyramidal units. The two-unit SBU is the “paddle wheel” motif associated especially with compounds like copper acetate. The zinc analog is a structural component of one of the earliest porous MOFs.<sup>33</sup> The four C atoms are the points of extension and are at the vertices of a square. Usually, as prepared, the Cu atoms have an additional ligand such as a water molecule forming square pyramidal coordination. This extra ligand can subsequently be removed, leaving “open metal sites”.<sup>34</sup>

The three-unit SBU is found in UMCM-150.<sup>35</sup> Here the points of extension form a trigonal pyramid.

An example with four metal-containing units is  $\text{Cd}_4(\text{CO}_2)_8\text{X}_4$  (here X is the O atom of DMF coordinated in the pyramid apical position).<sup>36</sup> Now the points of extension form a cube (perhaps better a tetragonal prism).

Figure 7 shows two SBUs long known as acetates, basic zinc acetate and basic chromium acetate.<sup>32</sup> They are now ubiquitous in MOF chemistry; early examples are in MOF-5<sup>37</sup> and in MIL-88, respectively.<sup>38</sup> For carboxylates, the composition is  $\text{OZn}_4(\text{CO}_2)_6$  and  $\text{OCr}_3(\text{CO}_2)_6\text{X}_3$  ( $\text{X} = \text{OH}/\text{H}_2\text{O}$ ). The points of extension form respectively an octahedron and a trigonal prism.

Figure 8 shows some SBUs with higher-coordination regular shapes. They are  $\text{OCO}_4(\text{CO}_2)_8$ ;<sup>39</sup> note the rather unusual square-planar coordination for the central O atom, a related SBU

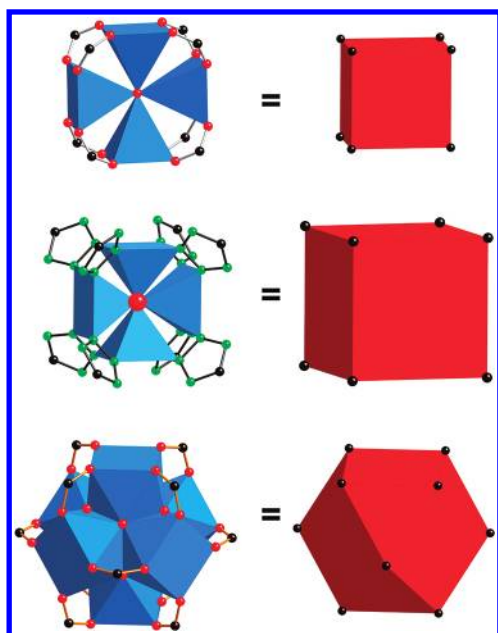


Figure 8. SBUs with (from top) eight, eight, and 12 points of extension.

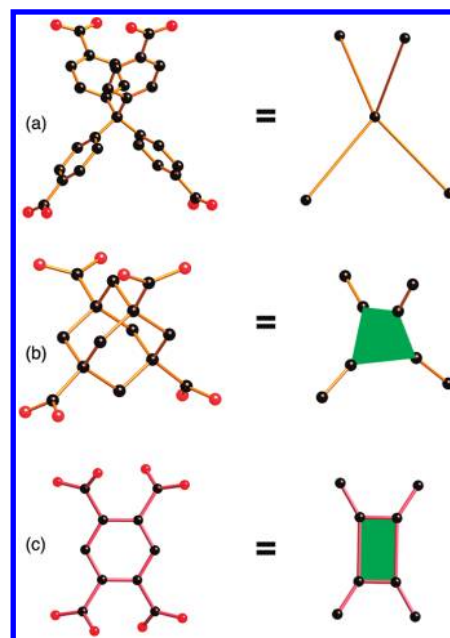


Figure 10. Examples of tetratopic linkers: (a and b) tetrahedral and (c) square.

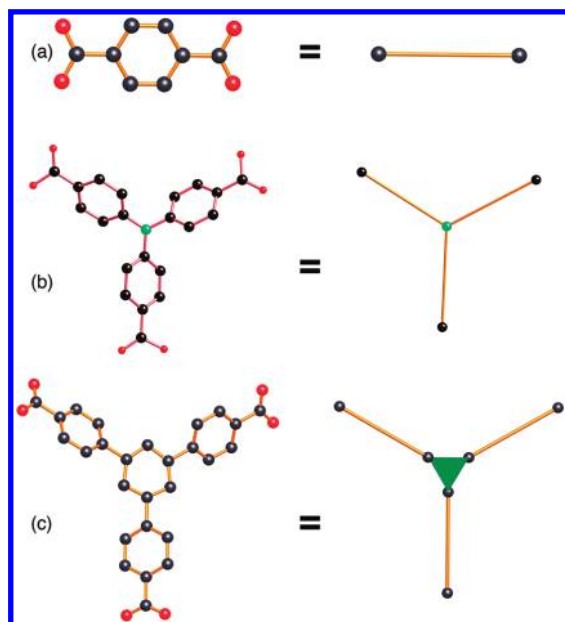


Figure 9. (a) A ditopic linker and (b and c) two tritopic linkers.

$\text{ClMn}_4(\text{tta})_8$  (here tta is a five-membered  $\text{CN}_4$  tetrazole ring part of a linker)<sup>40</sup> and  $\text{O}_4(\text{OH})_4\text{Zr}_8(\text{CO}_2)_{12}$ ,<sup>41</sup> in which the 12 C atoms that define the points of extension are at the vertices of a cuboctahedron.

#### 4.3. Some Simple Organic SBUs

Figures 9 and 10 show some commonly used carboxylate linkers. Notice that the two tritopic linkers in Figure 9 are considered to have the same “underlying” topology as do the two tetrahedral linkers in Figure 10 (recall the discussion in section 3). It is noted that linking the octahedral  $\text{Zn}_4$  unit of Figure 7 with the tritopic linker  $\text{N}(\text{C}_6\text{H}_4\text{CO}_2)_3$  (Figure 9b) yields MOF-150 with the expected edge-transitive (3,6)-c net

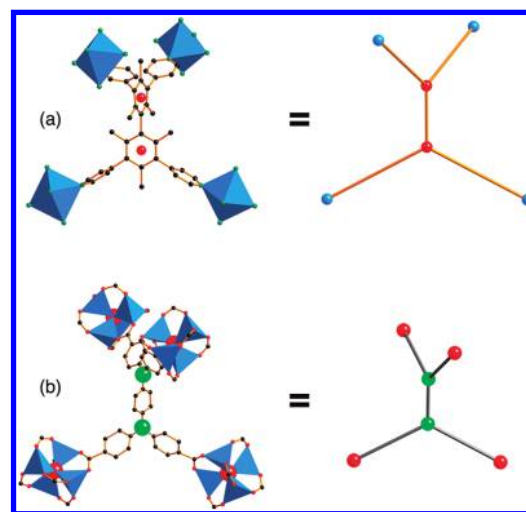


Figure 11. Two examples of octahedra or octahedral SBUs linked by tetratopic linkers in structures discussed in the text. Large spheres indicate 3-c branching points.

$\text{pyr}$ .<sup>42</sup> However, as a relatively rare exception to the predictability of linking simple shapes that is the basis for reticular chemistry, linking with the other tritopic linker in Figure 9c and with their longer derivatives produces an isorecticular series of MOFs (MOF-177, MOF-180, MOF-200) having the edge 5-transitive (3,6)-c topology **qom**. These are particularly attractive candidates for practical gas-storage applications.<sup>43</sup>

A tetratopic organic unit joined to octahedrally coordinated metal atoms is illustrated in Figure 11. The authors<sup>44</sup> recognized that the linker could be considered either as a single tetrahedral unit or as two triangular nodes; again the latter is preferred, as shown in the figure. It is noted in passing that the (4,6)-c net is **iac** net rather than what was described as (4,6)-c net “corundum” **cor**. The corresponding (3,6)-c net has the RCSR symbol **act**.

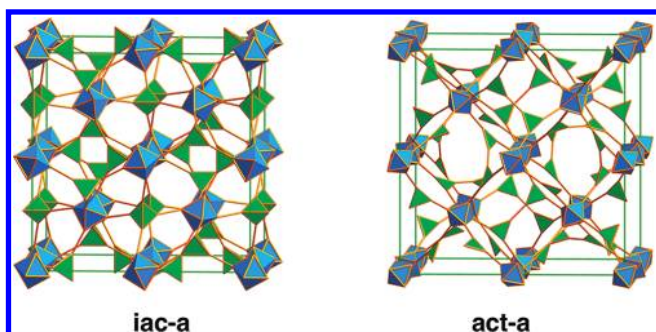


Figure 12. (4,6)-c (*iac*) and (3,6)-c (*act*) nets discussed in the text shown in their augmented forms.

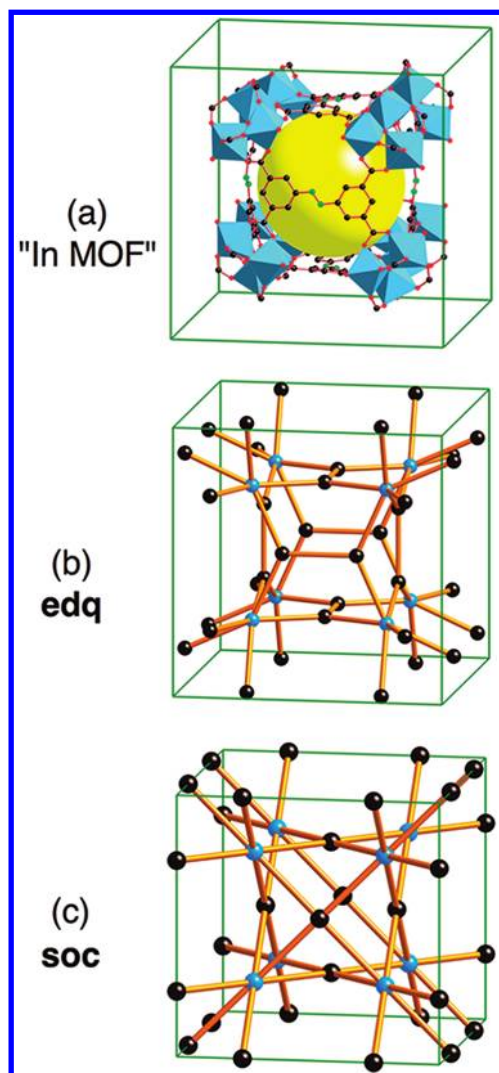


Figure 13. (a) a MOF (named “In MOF”) with a metal SBU with six points of extension linked by a tetratopic linker. (b) The preferred (3,6)-c net *edq* describing the underlying topology. (c) A (4,6)-c net (*soc*) alternatively used to describe the topology.

Curiously, the same misassignment (to *cor* rather than *iac*) was made in another example with a tetratopic organic linker (also shown in Figure 11) linked now to the  $Zn_4$  octahedral cluster of Figure 7.<sup>45</sup> Here again we prefer to consider the underlying

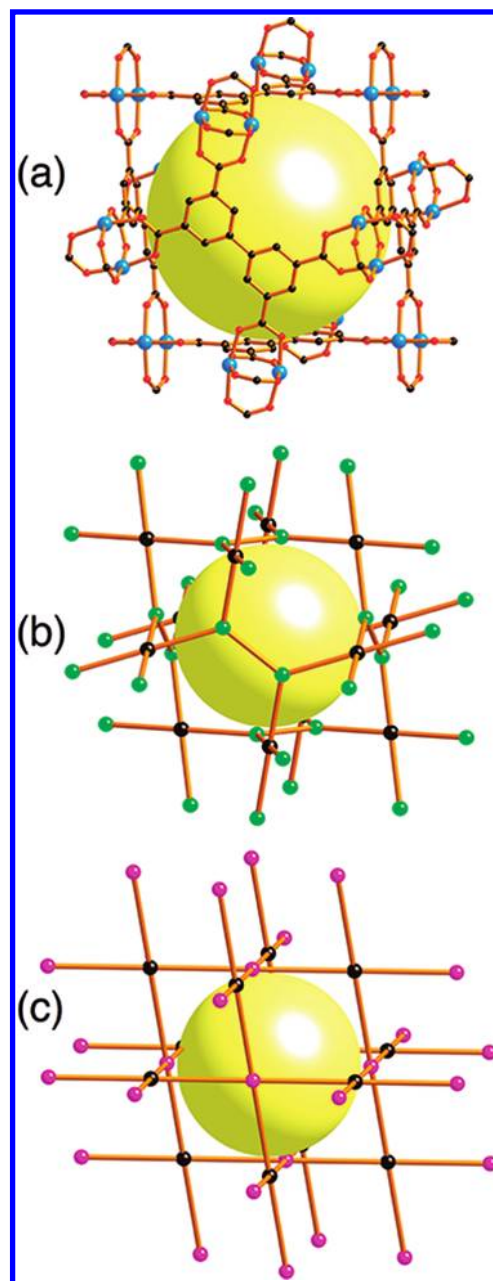


Figure 14. (a) MOF-505. (b) The underlying (3,6)-c net *fof*. (c) Showing how merging the 3-c vertices of *fof* produces the *nbo* topology.

topology as the (3,6)-c net *act*. The *iac* and *act* nets are compared in augmented form (*iac-a* and *act-a*) in Figure 12.

Another example of a MOF with the same kind of tetratopic linker is the “In MOF” shown in Figure 13.<sup>46</sup> The authors described the topology as that of the (4,6)-c net *soc*, but the description preferred here is of the (3,6)-c net *edq* (see Figure 13). The metal cluster SBU, which is composed of three  $InO_6$  octahedra, is discussed further below.

The same tetratopic linker was used to generate the structure of MOF-505 by linking  $Cu_2$  paddle wheels (Figure 14).<sup>47</sup> If the linker were to be considered as derived from one 4-c branching point (vertex) linked to the 4-c paddle wheel vertex, the underlying net would be the cubic 4-c net *nbo*, as shown in the figure. But again we prefer to consider the organic linker to have two 3-c vertices and the structure is then based on the (3,4)-c net *fof*. The

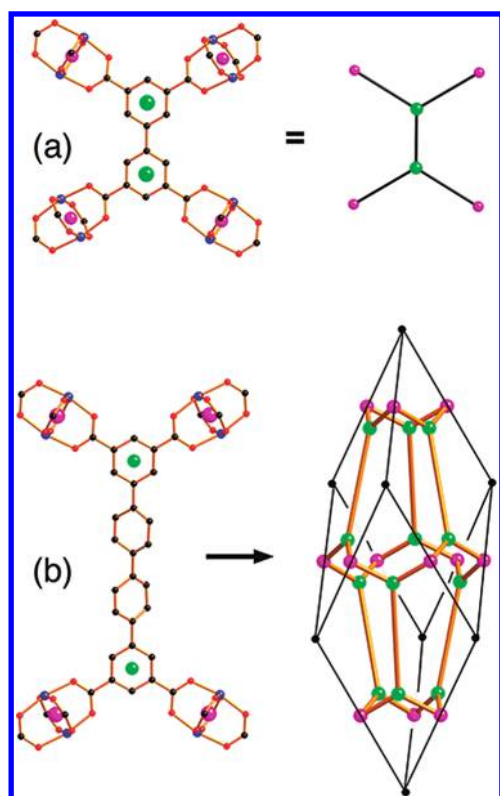


Figure 15. (a) Linker used in MOF-505 (Figure 14). (b) Linker in an isorecticular MOF. On the right is shown a primitive cell that would be cubic if the net were **nbo**.

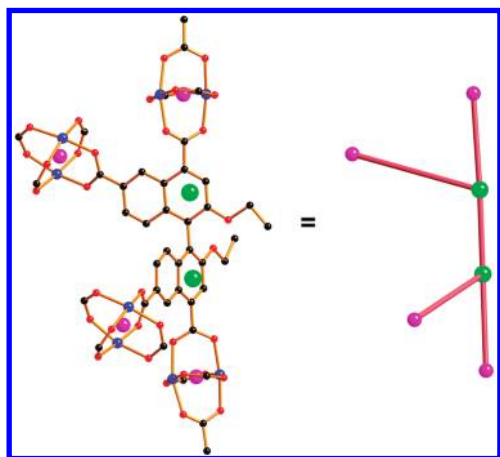


Figure 16. An example of a tetratopic linker. Large green balls indicate the location of 3-c branching points (vertices of the underlying net). The magenta balls are 4-c vertices of that net.

validity of the latter description becomes apparent when examining an isorecticular series derived from linkers with greater spacing between the 3-c vertices, as shown in Figure 15.<sup>48</sup> In these last examples, the structure deviates markedly from cubic metrics; the structures are actually rhombohedral and the axial ratios  $c/a$  are respectively for cubic **nbo**, MOF-505, and the two isorecticular analogs 1.22, 1.34, 2.07, and 2.84. Clearly, the last in particular is very far from cubic.

Our last example is a tetracarboxylate linker, which again we prefer to consider as having two 3-c branching point comes from an isorecticular series of chiral materials.<sup>49</sup> The linker is shown in

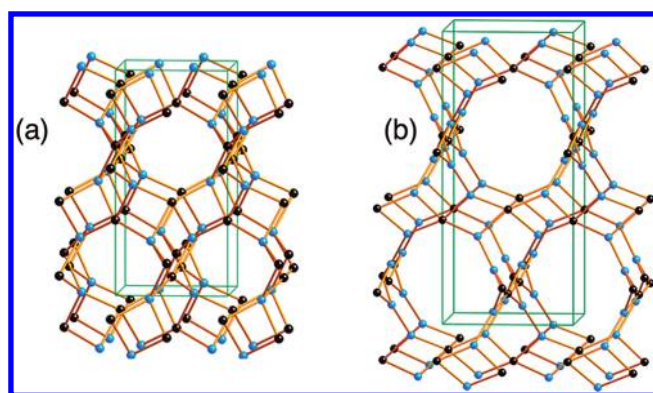


Figure 17. (a) The (3,6)-c net **wbl**. (b) The (3,5)-c net **lqm**.

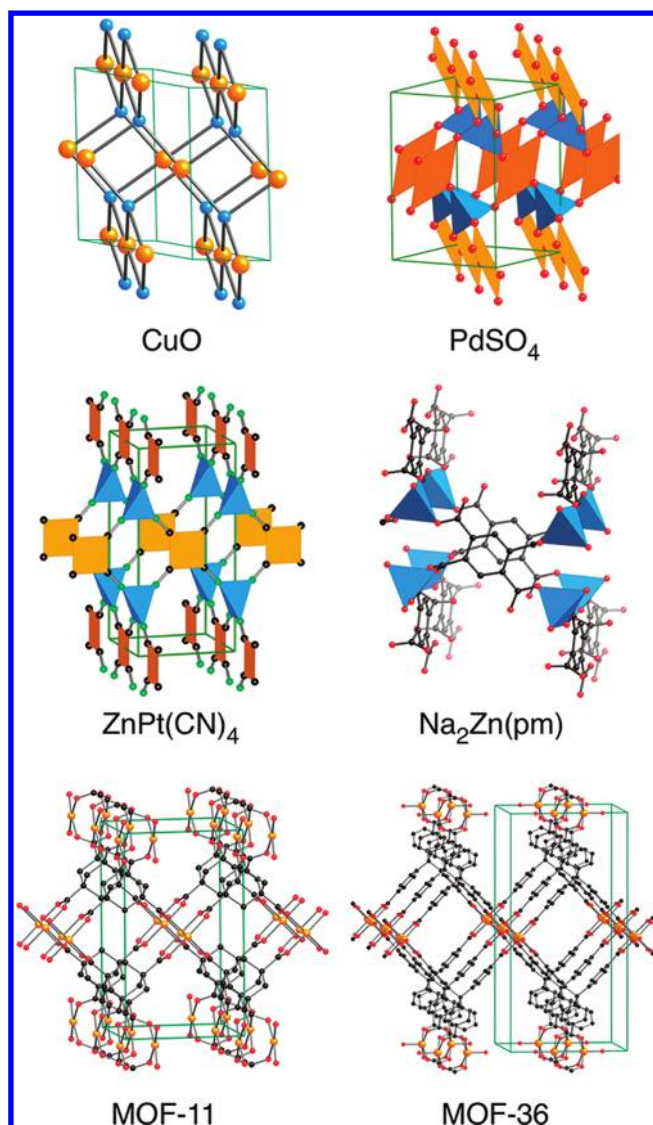
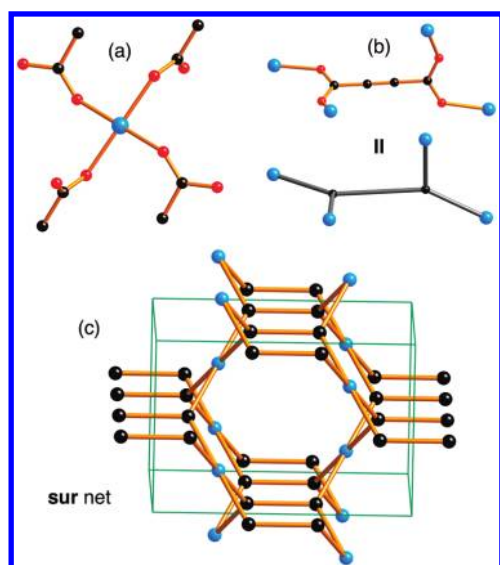


Figure 18. Some structures discussed in the text with the **pts** underlying net.

Figure 16. The authors preferred to consider the linker as a single 4-c vertex, and together with the 4-c paddle wheel vertex, the underlying net was described as a 4-c binodal net to which the RCSR symbol **wbl** has been assigned. However, in our



**Figure 19.** Fragments of the structure of hydrated zinc acetylene dicarboxylate. (a) Zn coordination to carboxylate O (coordinating water molecules not shown). (b) The acetylene dicarboxylate linker. (c) The resulting (3,4)-c net.

interpretation the underlying net is (3,4)-c (symbol **lqm**). Interestingly, both these nets are intrinsically chiral (symmetry  $I4_122$ ); they are compared in Figure 17. Note that the use of enantiopure ligands, as in this study, necessitates formation of enantiopure chiral crystals, regardless of the ideal symmetry of the underlying net. See section 5.6 for an example of chiral crystals produced with chiral ligands but with an achiral underlying net.

#### 4.4. Some Structures with the pts Topology

Figure 18 illustrates some structures with the 4-c net **pts** as underlying topology. CuO (tenorite) has a structure that is a monoclinic distortion of the tetragonal PtS (cooperite) structure. This allows the Cu atoms to have two more-distant O neighbors in addition to the four nearest neighbors completing a distorted octahedron. PdSO<sub>4</sub> also has a monoclinic structure, but the PdS arrangement, with  $-O-$  links, is topologically again **pts**.<sup>50</sup> Cyanides AB(CN)<sub>4</sub> with neutral or charged frameworks with the same (augmented) net have long been known and repeatedly rediscovered.<sup>51</sup> A atoms are tetrahedral cations such as Cu(I), Zn, Cd, and B atoms such as Cu(II), Ni(II), Pd(II), and Pt(II) with square-planar coordination.

An example of a compound (shown in Figure 18), again monoclinic, with tetrahedral metal and planar tetratopic linker is Na<sub>2</sub>Zn(pm)·xH<sub>2</sub>O, where pm = pyromellitate = benzene-1,2,4,5-tetracarboxylate (linker shown in Figure 10).<sup>52</sup> The Na ions are in the interstices of the charged Zn(pm) framework. Notice that only one of each two carboxylate linkers is bonded to Zn. Compounds of this sort (reported in 1882) with charged frameworks and counterions in the channels may be considered as forerunners to the later MOFs with neutral frameworks and permanent porosity. The author did note that the structure was “zeolite-like”.

Also shown in Figure 18 are early examples, MOF-11<sup>34a</sup> and MOF-36,<sup>34b</sup> of neutral-framework MOFs with the **pts** topology. These combine the paddle wheel metal-containing SBU in Figure 6 with one or other of the tetrahedral linkers of Figure 10. The volume increase from PdO to MOF-36, which have the same symmetry, is a factor of 66.

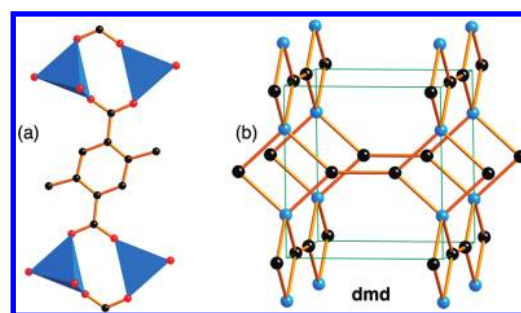


**Figure 20.** (a) A fragment of the structure of zinc dimethyl benzene dicarboxylate. (b) The (3,4)-c net that would result if the Zn atoms were taken as tetrahedral vertices and the tetratopic linker taken as having two 3-c vertices (see the text).

#### 4.5. Two MOFs Whose Preferred Description Is Not the pts Topology

Here we discuss two MOFs to which Alexandrov et al.<sup>26</sup> assign the **pts** topology but for which we prefer an alternative description. The first is a hydrated zinc acetylene dicarboxylate.<sup>53</sup> The zinc ions are six-coordinated, to two water molecules and to four carboxylate O atoms from different carboxylate groups, so the latter form four points of extension at the vertices of a square (Figure 19). The organic linker has a tetrahedral envelope, so Alexandrov et al.<sup>26</sup> identify the underlying net as **pts**. But as described in section 4.3, we prefer to consider such a linker as having two 3-c vertices and the net to be the (3,4)-c net **sur**, as shown in the figure.

The second example is a zinc salt of dimethyl benzenedicarboxylic acid<sup>54</sup> shown in Figure 20. Now the Zn is tetrahedrally four-coordinated, and the tetratopic linker has a planar envelope, so taking Zn atoms and the center of the linker as vertices, Alexandrov et al.<sup>26</sup> again get the 4-c **pts** net. But, as in the previous case, we would prefer to consider the linker as having two 3-c vertices. If the Zn atoms are retained as 4-c nodes, we would again get a (3,4)-c net, now **dmd** (Figure 20). But in this case we note that the Zn atoms share points of extension so in fact we really prefer a third description in which the metal cluster SBU is an infinite rod of Zn atoms linked by carboxylates. The linker from this point of view is ditopic, more consistent with the earlier discussion. We give this description in section 6.3

#### 4.6. MOFs with Multiple Links between SBUs

Occasionally one finds structures in which two or more linkers run parallel and join the same pair of vertices. Three examples are illustrated here. It is generally agreed that crystal nets do not admit multiple edges, so it is probably best in most cases to consider these as just one edge, although in some instances a pair of edges joining two SBUs can be abstracted as part of a rectangle, as shown here.

The first involves an elegant SBU with composition SiO<sub>4</sub>Zn<sub>8</sub>(CO<sub>2</sub>)<sub>12</sub> with the 12 C atoms acting as points of extension.<sup>55</sup> In one example of this SBU the linkers are bdc = terephthalate = benzene-1,4-dicarboxylate, so the framework has composition SiO<sub>4</sub>Zn<sub>8</sub>(bdc)<sub>6</sub>.<sup>55</sup> As shown in Figure 21, pairs of parallel linkers join pairs of SBUs, so each SBU is linked to six others as in a primitive cubic lattice (**pcu** net), and this is one way of describing the topology. However, if we consider the 12 points of extension separately, it may be seen in the figure that the topology is that of icosahedra linked to six others by rectangles (squares in the illustration). This second description corresponds to the uniodal 6-c net **snf**.

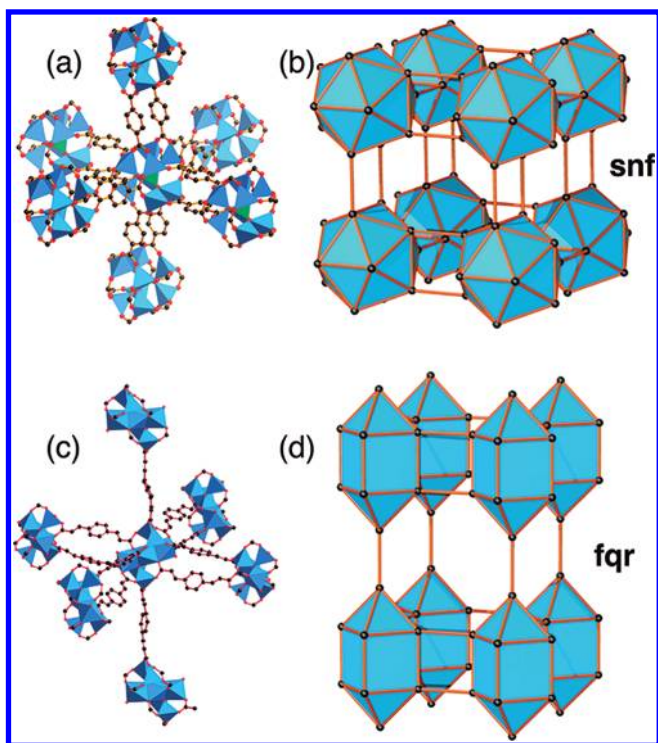


**Figure 21.** MOFs with multiple links between pairs of SBUs. (a) An SBU linked to six others by pairs of links. (b) The net obtained if pairs of linkers are considered sides of quadrangles. (c) An SBU linked to four others by pairs of links. (d) The net obtained if pairs of linkers are considered sides of quadrangles.

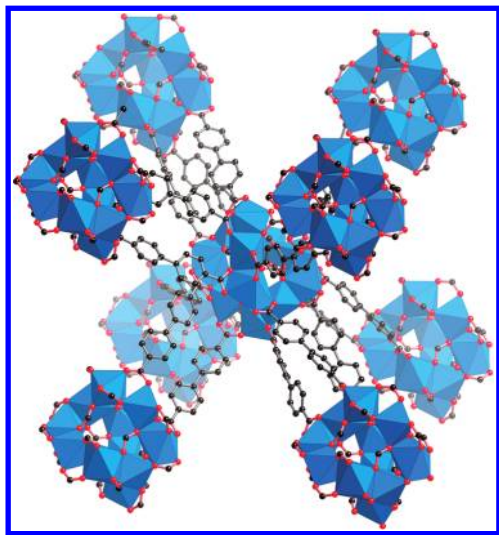


**Figure 22.** A MOF with an SBU with 18 points of extension and multiple links between pairs of SBUs. Each SBU is linked to eight others.

The second example has a related structure. Now the metal cluster SBU with stoichiometry  $Zn_7O_4(CO_2)_{10}$  has 10 points of extension and is linked to six other SBUs—to four by double links and to two by single links.<sup>56</sup> Again the double links may be abstracted as rectangles and the net described as the 5-c net **fqr**, as shown in Figure 21.

A third example is a structure in which the metal-containing SBU consists of 11 Cd atoms and which has 18 points of

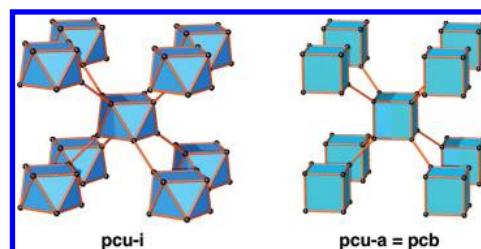


**Figure 23.** Two nets with the same underlying topology (**bcu**).

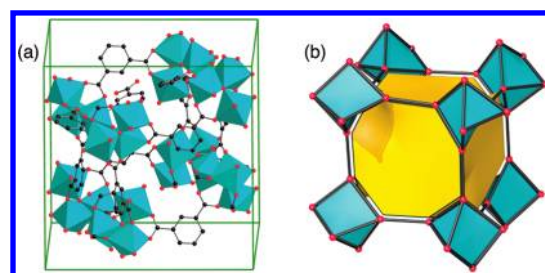


**Figure 24.** A MOF with trigonal-prism SBUs linked with primitive cubic (**pcu**) topology: (a) a unit cell of the structure and (b) the trigonal prisms linked in **pcu** topology. The net of the vertices (red) is the uninodal 4-c **unp**.

extension, again carboxylate C atoms, now of biphenyl dicarboxylate (**bpdc**).<sup>57</sup> The Cd cluster, formed from 11  $CdO_6$  octahedra, also contains formate ( $HCO_2$ ) groups that serve to hold the cluster together, and the framework is formulated as  $Cd_{11}(HCO_2)_6(bpdc)_9$ . In this structure, each cluster is linked to eight neighboring clusters—to each of two by three **bpdc** linkers and to the other six by pairs of linkers (Figure 22). Considering the multiple links between a given pair of SBUs as one edge and the clusters as 8-c vertices, the net is body-centered cubic (**bcu**). In this case, there is no obvious alternative description. Notice that the cluster is chiral and has ideal symmetry  $32 (D_3)$ ; the crystal symmetry is the achiral  $R3c$ , which means that clusters of both hands occur equally.

#### 4.7. Examples of Lower-Symmetry Metal-Containing SBUs

It was remarked earlier that the augmented net derived from an underlying net was not strictly defined in a mathematical sense. For example, if one takes any polyhedron with eight vertices and links it to eight neighbors in the same way topologically as in **bcu** (the net of the body-centered cubic lattice), the derived net will have **bcu** as its underlying net. This is illustrated in Figure 23 using the net **bcu-i**, in which square antiprisms are linked in such a way. Clearly, the net is different (5-c, symmetry  $I422$ ) from **bcu-a** (4-c, symmetry  $Im\bar{3}m$ ), but the underlying net is the same.

Such examples are quite common in crystals. Figure 24 shows an example of an SBU that has points of extension at the vertices of a trigonal prism linked with the **pcu** topology by bent ditopic linkers. The SBU is in fact the same as that shown in Figure 13 and the authors correctly identified the underlying topology as **pcu**.<sup>46</sup> The “augmented” 4-c net shown in Figure 24 has the RCSR symbol **unp**.

An example with a square antiprism replacing a cube is found in the structure of a cyanide with framework composition  $Fe_2(H_2O)_4Mo(CN)_8$ , with Fe bonded in a planar fashion to four

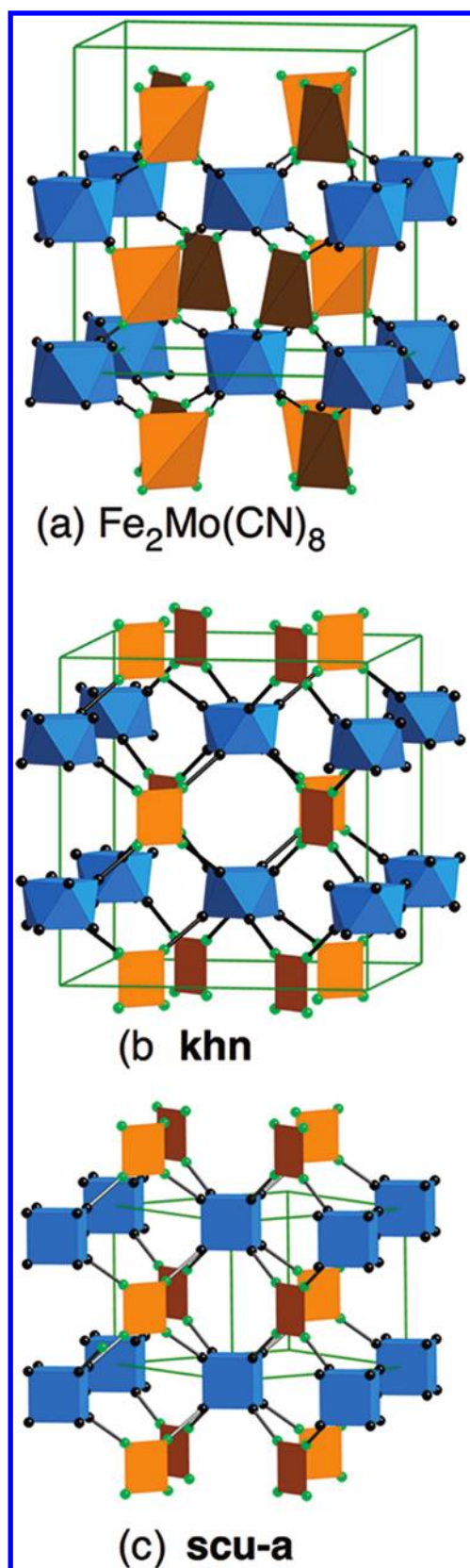


**Figure 25.** (a) The framework of a Fe, Mo cyanide with  $\text{MoC}_8$  square antiprisms and  $\text{FeN}_4$  quadrangles (two water molecules coordinating the iron atoms not shown). (b) The net **kh<sub>n</sub>** of the linked C and N atoms. (c) The net **scu-a** of the augmented **scu** net.

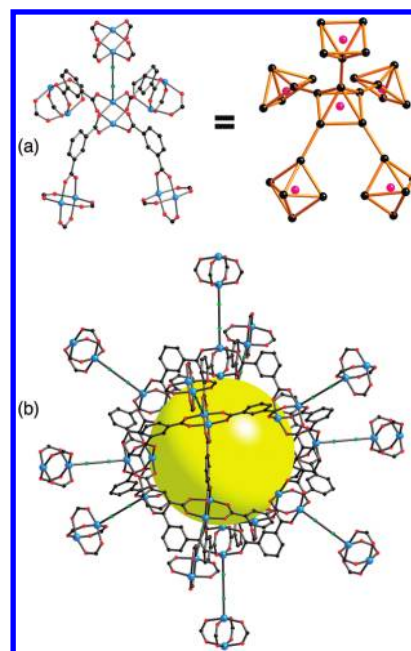


**Figure 26.** (a) Fragment of a MOF with Zn square paddle wheel SBUs linked by methyl isophthalic acid (methyl groups not shown in the figure). (b) Twenty-four SBUs form MOP-1 clusters that are further linked by dabco linkers (abstracted as linear ditopic linkers in the drawing).

CN groups and with two water molecules completing an octahedron (Figure 25).<sup>58</sup> The net of the linked antiprism and square is a (3,5)-c net with RCSR symbol **kh<sub>n</sub>** and symmetry  $I4/mcm$ . The underlying net is the (4,8)-c net **scu**, shown in its most symmetrical augmented form as linked squares and cubes in the figure. It may be noted that the  $\text{FeN}_4$  “squares” in Figure 25 are not strictly planar and might be construed as tetrahedra; the underlying net would still be the same.

## 5. SOME CASE STUDIES

### 5.1. A MOF with **ubt** Topology

Another example discussed by Alexandrov et al.<sup>26</sup> is a crystal of linked paddle wheels reported by Chun.<sup>59</sup> In this material, the four points of extension of the  $\text{Zn}_2(\text{CO}_2)_4$  paddle wheel are linked to methyl isophthalic acid. One of the Zn atoms is also connected to a ditopic dabco linker to make the unit a node of a 5-c net. This is illustrated in Figure 26 (note that in this figure the structure is somewhat simplified by omitting nonessential atoms for clarity). Alexandrov et al. propose several different interpretations of the topology. One considers the two Zn atoms of the SBU as separate 4-c and 5-c vertices of a net. But this is not consistent with our general procedure which considers all metal atoms with common points of extension (carboxylate C atoms in this case) as part of one cluster. A second possibility is to consider the topology as simply defined by linked 5-c vertices, as shown in Figure 26. This is sufficient to define the topology completely as the net is the uninodal net **ubt** (so named as it is the B net in  $\text{UB}_{12}$  as Chun recognized).

However, there is more to this structure. The  $120^\circ$  angle between the carboxylates of the linker is just right to make a closed polyhedron from 12 paddle wheel units. Such a supercluster is indeed found in the metal–organic polyhedron MOP-1.<sup>60</sup> The

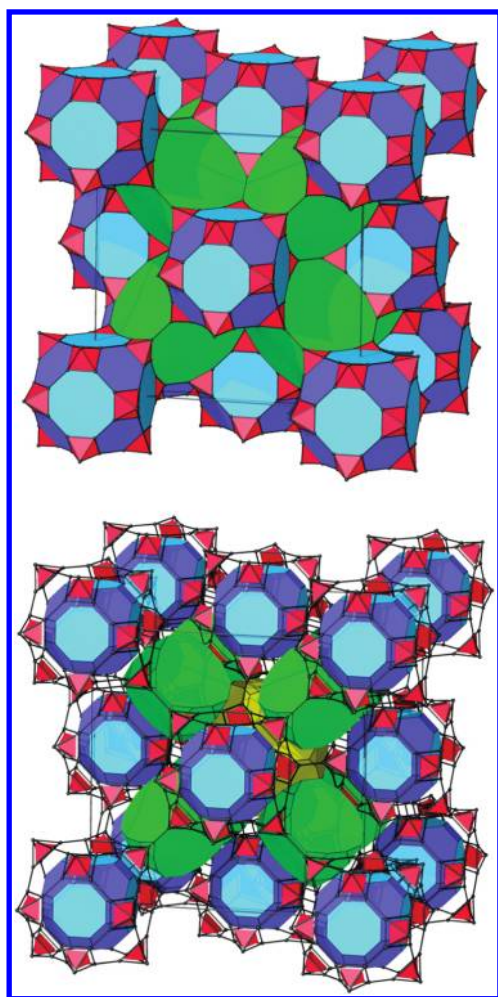


**Figure 27.** The augmented **ubt** net as a tiling. In the lower half, the tiles are slightly shrunk to leave gaps between them. Red tiles are square pyramids.

12 outer Zn atoms of this supercluster are also joined to the ditopic dabco linker so the MOP units are linked into a 12-c net which is in fact the net, **fcu**, of the face-centered cubic lattice (note that **ubt** can also be symbolized **fcu-a**), and Alexandrov et al. propose this as an alternative description of the underlying net. But this is not admitted here as the separate paddle wheels do not have common points of extension and should be considered separately. Interestingly, this structure was recently rediscovered with 4,4'-bipyridine linking MOP-1 units, and this was described as based on the **fcu** net.<sup>61</sup>

The net of the points of extension taken as separate vertices is the augmented net **ubt-a**. This is illustrated in Figure 27 as the net of a tiling. In the figure the blue “MOP” units are in a face-centered cubic array and the green and yellow tiles correspond respectively to the tetrahedral and octahedral holes of that lattice. We remark that the tiling is not *natural* in this case, as the square pyramid tile has one face larger than the rest.<sup>13a</sup>

## 5.2. MOFs with Hexatopic Carboxylate Linkers

A particularly interesting isorecticular series of MOFs has emerged in the past few years, although there has been no general agreement on the best description of the topology. The topology was first found independently and essentially

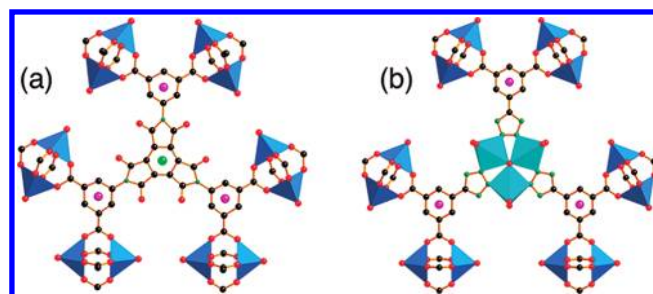


**Figure 28.** (a) A hexatopic linker joined to paddle wheel SBUs. Blue shapes are Zn–O (left) coordination polyhedra. Large green and magenta spheres mark 3-c vertices of the net. (b) Another hexatopic linker now linked to Cu paddle wheels. The light blue shapes are  $\text{CuN}_2\text{O}_3$  trigonal prisms. The central O atom is a 3-c vertex corresponding to the green sphere in part a.

simultaneously by two groups.<sup>62</sup> There have been several subsequent syntheses that have produced isorecticular materials, some with exceptional porosity.<sup>2a,63</sup> The topology has been identified as the **ubt** structure described in section 5.1 and also described as the (3,24)-c net **rht**. A different assignment is made here.

Figure 28 shows the linked metal-containing (Zn or Cu carboxylate paddle wheels) and organic SBUs for two compounds. Note that in one case the “organic” component is actually a hybrid metal–organic SBU.<sup>62a</sup> In each case, the center of the unit is a 3-c branching point (vertex) of the net, and in each case the magenta spheres in the figure are also 3-c vertices. The centers of the paddle wheels are, as usual, 4-c vertices. The resulting net, RCSR symbol **ntt**, is a trinodal (3,4)-c net. Note that, as in the previous section, the paddle wheels are again linked by metadicarboxylate units and the structure again contains the MOP-1 cluster of 12 paddle wheels (Figure 29). Now, however, these units are joined by links to the 24 edges of that cluster, hence having the alternative description of a (3,24)-c underlying net (RCSR symbol **rht**).

If the arms of the linker are made shorter, it is no longer possible for the links to 3-c vertices in a given SBU to be all planar. Then another trinodal (3,4)-c net, symbol **zyg**, is found.<sup>64</sup> Interestingly, this net, like **ntt**, has the minimum number, two, of different kinds of edge (Figure 29); in the jargon the nets are edge two-transitive. The linker is the same as the one shown in Figure 31 below.

Yet another point of interest about the **ntt** topology is what happens if one considers the hexatopic organic unit to be just one hexagonal 6-c vertex in the same way as suggested by Alexandrov et al.<sup>26</sup> for the tetatopic SBU in Figure 11 (section 4.3). Then one obtains an edge-transitive (4,6)-c net. This net is not in our compilation of such nets<sup>13e,14</sup> for the following reason. As may be seen from Figure 30, pairs of 4-c vertices have the same set of four neighbors. As a consequence, in barycentric (center-of-mass) coordinates the 4-c vertices collide in pairs. More importantly, such a graph has “non-rigid body” symmetries; thus, interchanging a pair of vertices with common neighbors while the rest is kept unchanged is a symmetry (automorphism) of the graph. Such an operation cannot correspond to a rigid body symmetry operation and the automorphism group of the net does not correspond to a crystallographic symmetry group. For this reason, such nets are often called “noncrystallographic”.<sup>65</sup> There is no compelling reason to avoid such nets, but when possible, an

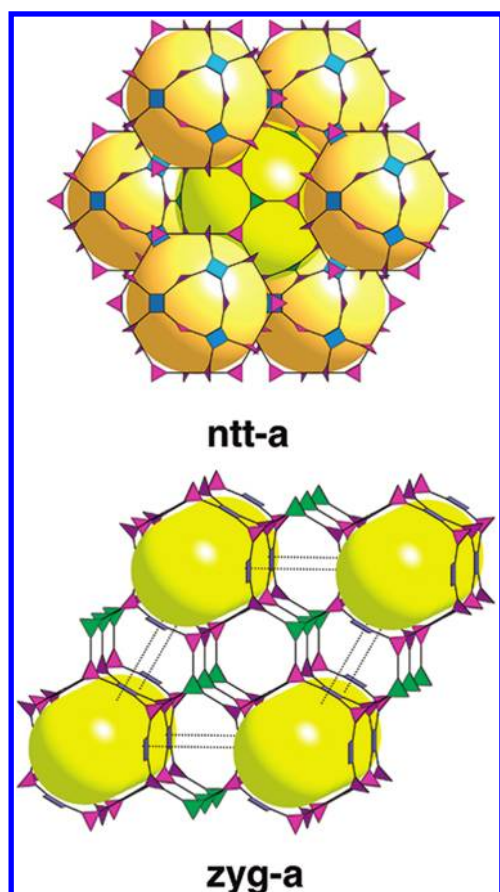


Figure 29. Augmented versions of two trinodal (3,4)-c nets discussed in the text.

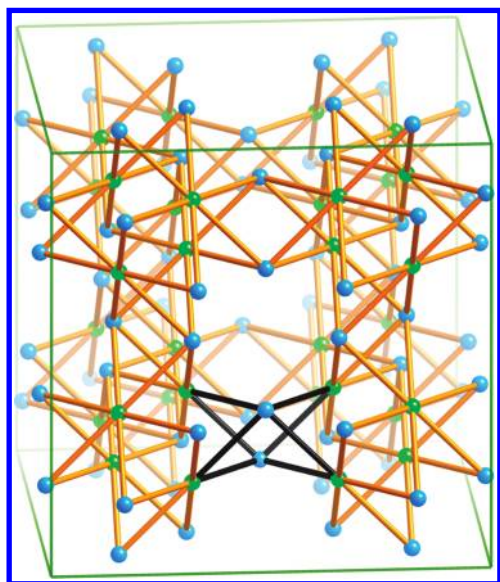


Figure 30. A net with noncrystallographic symmetries. Notice that the black links join each of a pair of blue vertices to the same set of four green vertices.

alternative topological description is preferred when they arise. More to the point perhaps is that the net in Figure 30 does not really reflect the nature of the parent structures.

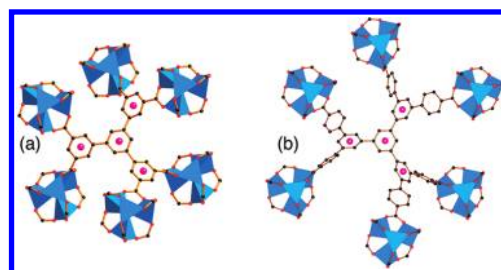


Figure 31. Units of the structures of two MOFs: (a) ref 66 and (b) ref 67. In both cases, 3-c vertices (branching points) are shown as large magenta spheres and 6-c vertices are at the center of the cluster of four  $\text{ZnO}_4$  tetrahedra (blue).

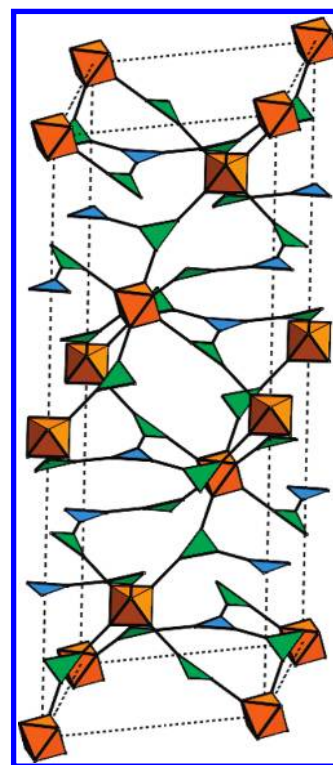


Figure 32. The (3,6)-c net **zxc** shown in augmented form (**zxc-a**) as linked triangles and octahedra.

The corresponding edge-transitive (4,6)-c net derived from **zyg** is the binodal edge-transitive net **stp**.

The small tetratopic linker that led with paddle wheels to the **zyg** topology has also been linked to the octahedral basic zinc acetate SBU, as shown in Figure 31.<sup>66</sup> Now one gets a trinodal (3,6)-c net **zxc** shown in augmented form in Figure 32. This net also has the minimum number of kinds of edge, emphasizing again that the most simple possibility is often what is obtained in practice. Interestingly, when the linker is expanded, as shown in Figure 31, the same topology is found with the same Zn SBU.<sup>67</sup> It would be interesting to see if further isorecticular compounds could be made using some of the other linkers of this section.

It should be apparent from Figure 31 that the envelope of the organic linker is an octahedron, and if this were adopted as a basic unit, then the underlying net would be 6-c with octahedral metal SBUs joined by octahedral linkers. In fact, it has the topology of a binary version of the primitive cubic net **pcu** as in NaCl, and this

Scheme 1

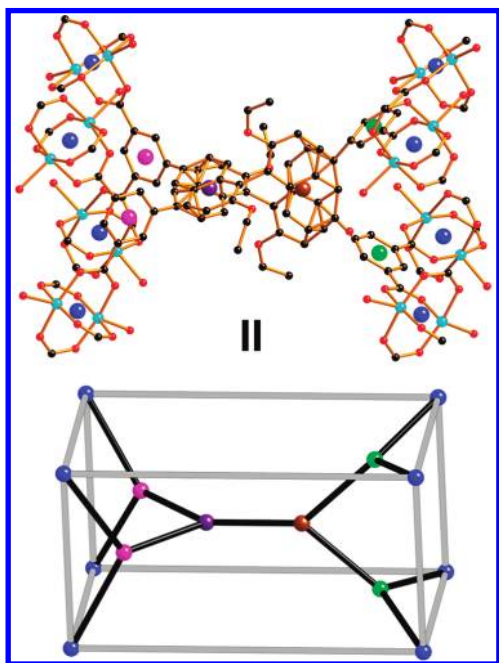
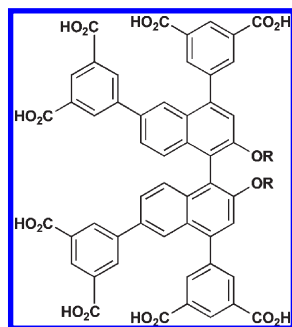


**Figure 33.** Deconstruction of a MOF described in the text. The octatopic linker is considered to contain six 3-c branching points (vertices) linked to eight 4-c vertices (blue balls) in the center of copper paddle wheels. Vertices in different colors are unrelated by symmetry in the crystal structure (but not necessarily in the net).

description was preferred by both sets of authors.<sup>66,67</sup> But, although informative, this does not explain the far from cubic metrics of the crystal structures.

### 5.3. MOFs with Octatopic Linkers

An isorecticular series of MOFs has been made by linking paddle wheels by octatopic carboxylate linkers of the type shown in Scheme 1.<sup>68</sup> We take a unit of one of these directly from the CIF file reported in the paper to illustrate how we deconstruct the framework. We note that, as is very commonly the case in MOF structures, there is considerable disorder of the carbon atoms. In this case, although the paddle wheels are clearly resolved, the center of the organic linker is disordered. However, it is easy enough to locate the branching points shown as spheres in Figure 33. In the real structure with symmetry  $P4$  there are four different 3-c points identified by different colors in the figure and one 4-c point (all the paddle wheels are related by symmetry). When these vertices and their edges are submitted to Systre, it is

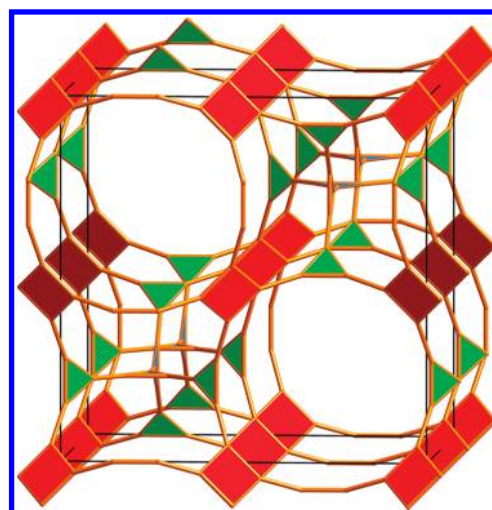


**Figure 34.** The augmented version (**mml-a**) of the (3,4)-c net **mml**.

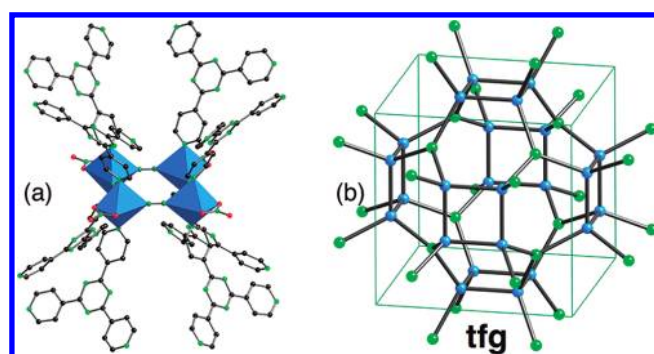


**Figure 35.** (a) A group of four single-metal-atom SBUs, each with four points of extension, linked to tritopic linkers. (b) The underlying net.

found that in fact the net is a trinodal (3,4)-c net that has been assigned the RCSR symbol **mml** with symmetry  $P4/nmm$ . The details of the calculation are given in this case in the Supporting Information as an aid to beginners at analyzing topology. The net **mml** is shown in augmented form **mml-a** in Figure 34. As shown in Figure 33, the envelope of the organic linker is a tetragonal prism and indeed if that group were simplified to an 8-c node the net would be the (4,8)-c net with RCSR symbol **scu** as the authors recognized.

### 5.4. More on Metal Cluster SBUs

In sections 5.1 and 5.2 the idea of using a supercluster of 12 paddle wheel SBUs as a single component of the underlying topology was rejected. It is proposed that to count a metal-containing cluster as a single SBU, the metal atoms must share (have direct connection to) a point of extension. Here another example is considered with that guideline applied. This is a structure composed of  $Zn_4(CN)_4(NO_3)_4$  units joined by tritopic coordinating linkers (Figure 35).<sup>69</sup> Here, four octahedrally coordinated Zn atoms are linked into a square by CN links. As we consider C–N groups also to be linkers, the individual octahedra should be considered as the metal SBUs. Two of the octahedral vertices are occupied by O of nitrate groups and thus not points of extension. The result is then that we have 4-c vertices joined by ditopic linkers (the CN groups) and tritopic linkers into a (3,4)-c net with RCSR symbol **tfg** (Figure 35) as described by the authors. In the real material two such nets interpenetrate.

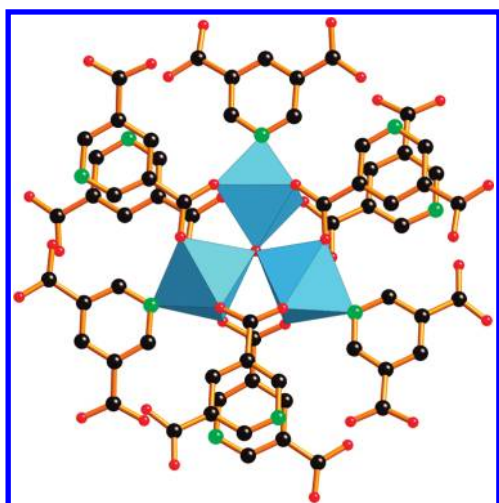


**Figure 36.** An SBU with nine points of extension: six carboxylate C atoms (black) forming a trigonal prism and three capping nitrogen atom (green).

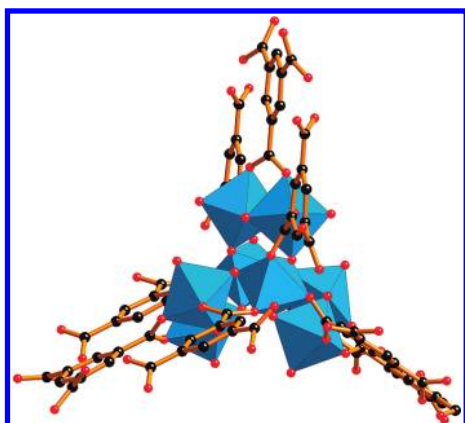


**Figure 37.** An SBU formed from eight  $\text{AlO}_6$  octahedra with nine points of extension (carboxylate C atoms, black).

Two examples of a 9-c SBU were reported at the same time.<sup>70</sup> In this the three “unused” octahedron vertices of the trigonal-prismatic basic Cr acetate SBU shown in Figure 7 are also utilized as points of extension. One example is provided by the SBU  $\text{OCo}_3(\text{CO}_2)_6\text{N}_3$  (Figure 36). Here the 6 C and 3 N atoms are the points of extension forming a tricapped trigonal prism. Each N atom is part of the tritopic linker pyridine-3,5-dicarboxylate.<sup>68</sup> A second example has Fe replacing Co in the SBU and an expanded linker, pyridine-3,5-bis(phenyl-4-carboxylate), producing an isorecticular material.<sup>70b</sup> The underlying topology is a simple binodal (3,9)-c net **xmz** formed by the 9-c metal cluster SBU and the 3-c organic linker. This net has the minimum possible kinds of edge, two (it impossible to have nine equivalent edges meeting at the 9-c vertex, as there is no symmetry operation of order nine in a three-periodic structure).

Another SBU with nine points of extension is found in MIL-110.<sup>71</sup> The SBU has composition  $\text{Al}_8(\text{X})_{15}(\text{CO}_2)_9$  ( $\text{X} = \text{OH}, \text{H}_2\text{O}$ ) and the linker is trimesate (1,3,5-benzenetricarboxylate) (Figure 37). The SBU is a chiral assembly of eight  $\text{AlO}_6$  octahedra with symmetry  $32 (D_3)$  with similarity to the  $\text{Cd}_{11}$  cluster of Figure 22. The 9-c SBU together with the 3-c trimesate linker form another binodal (3,9)-c net **gfy** that again has the

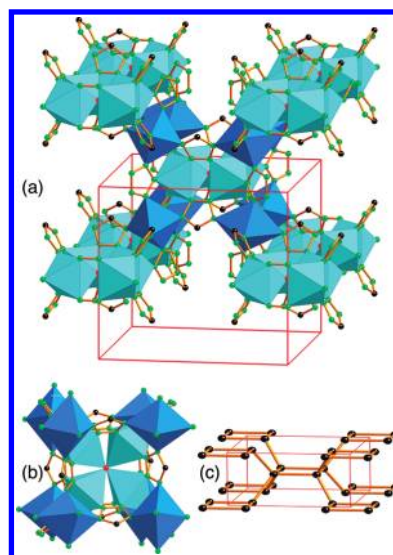


**Figure 38.** (a) A MOF with an SBU composed of  $\text{CuNO}_6$  octahedra (light blue) with four points of extension forming a square. These are lined by  $\text{CuN}_6$  octahedra (dark blue) acting as ditopic linkers. (b) How the light blue square in it is linked by eight edges (dark blue). (c) The 4-c net **crb**.

minimum possible number of edges. The net symmetry is  $P6_3/mmc$  but because of the chiral SBU the crystal symmetry is  $P6_322$ .

Our last example of a metal cluster SBU in this section is one that is essentially 2-c and so serves as part of an edge rather than as a branching point (vertex) of a net. The compound has a framework of composition  $\text{Cu}_8\text{O}(\text{tta})_{12}$  ( $\text{tta} = \text{tetrazolate}$ ) with perchlorate counterions.<sup>72</sup> The Cu atoms are of two kinds, half are in  $\text{CuN}_5\text{O}$  octahedra, four of which share a common O vertex. These are shown as dark blue in Figure 38. Linking these groups are  $\text{CuN}_6$  octahedra (light blue). Each dark blue octahedron is linked to just two light blue ones so we consider it part of an edge. The light blue octahedra are linked to two dark blue octahedra and to two light blue octahedra and thus act as 4-c vertices of the net, which is the simple uninodal **crb** net (also shown in the figure). Notice that here we omit the linking of diagonally opposite Cu atoms of the four-Cu-atom unit by the central O atom.

### 5.5. More Structures with Linked MOPs

In section 5.1 and 5.2 we met structures in which 12  $\text{Cu}_2$  square paddle wheels were linked into MOP-1 units. Here we adduce two more examples which have some fascinating topologies. The MOP-1 structure consists of 12 paddle wheels with their centers at the vertices of a cuboctahedron. The carboxylate C atoms (the points of extension) form a truncated cuboctahedron, as shown in Figure 39. The centers of the edges of that polyhedron, shown as blue balls in the figure, correspond to 3-c branching points when the MOPs are linked as in the series of section 5.2 with **ntt** topology. These last points are at the vertices of a rhombicuboctahedron, an Archimedean polyhedron with 24 vertices. When the MOPs are linked, these points and the centers of the paddle wheels are 4-c vertices of the underlying net, as shown in the figure.

In the MOFs considered here, the authors chose to consider the vertices of the net just the organic branching points (large blue spheres in Figure 39), so the MOP is abstracted as a rhombicuboctahedron.<sup>73,74</sup> In both cases, square faces of one are linked to square faces of another by four links so that overall

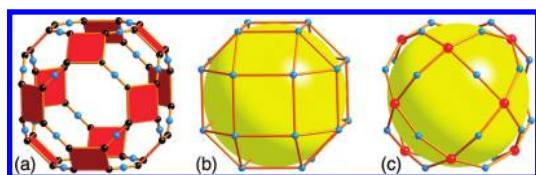


**Figure 39.** Three aspects of the MOP-1 topology. (a) Twelve linked squares with blue balls marking the points of extension when MOPs are linked into frameworks. (b) The pattern (a rhombicuboctahedron) of just those points of extension. (c) The pattern of 4- and 3-c vertices in a linked framework.

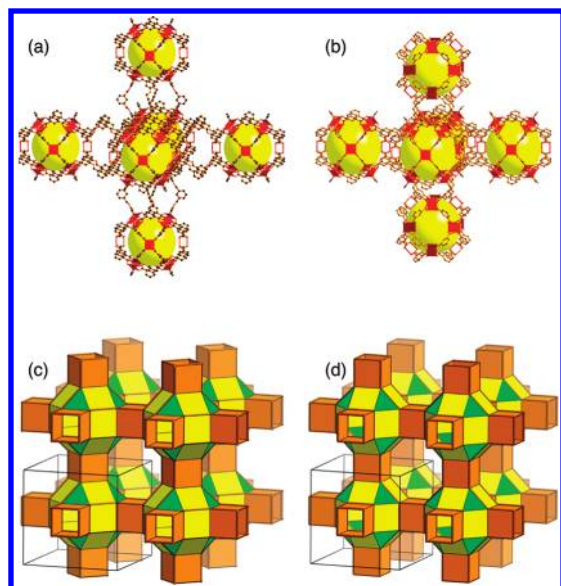


**Figure 40.** (a and b) Structures formed by linking MOPS to six others. (c and d) The nets produced by just the points of extension (blue in Figure 39 in parts a and b, respectively). The nets of the structures are **mjz** (c) and **pcu-i** (d).

each MOP is connected to six others, as shown in Figure 40. The array of MOPs form a primitive cubic array. The most symmetric way to do this results in a uninodal 5-c net, **pcu-i**, of cubic symmetry.<sup>73</sup> In the other structure the net of organic branching points, **mjz**, is binodal and has tetragonal symmetry, as shown in the figure.<sup>73</sup> These two nets are generated by linking rhombicuboctahedra by cubes. We can also consider the nets as a tiling of a 3-periodic surface by polygons (“infinite polyhedra” or *apeirohedra*) with one triangle and four squares meeting at every vertex, so the two-dimensional vertex symbol is  $3.4^4$  in both cases. Note we use a vertex symbol appropriate for a two-dimensional tiling of the infinite surface; for the three-dimensional 5-c net, the vertex symbol for **pcu-i** is  $3.4.4.4.4.8.8.8.8$ , indicating that there are eight rings in the net. Readers unfamiliar with vertex symbols are referred to a recent review.<sup>24</sup>

However, the description in the previous paragraph is insufficient to fully describe the topology of these structures. In the MOP rhombicuboctahedron, there are two kinds of square, say A and B. One, say A, contains the 4-c net vertex and the other does not. In the structures described above the first has, per MOP, one AA and two BB links between MOPs. The resulting (4,5)-c net is assigned the RCSR symbol **zmj**. We believe this best describes the underlying topology of the MOF. The second structure has one

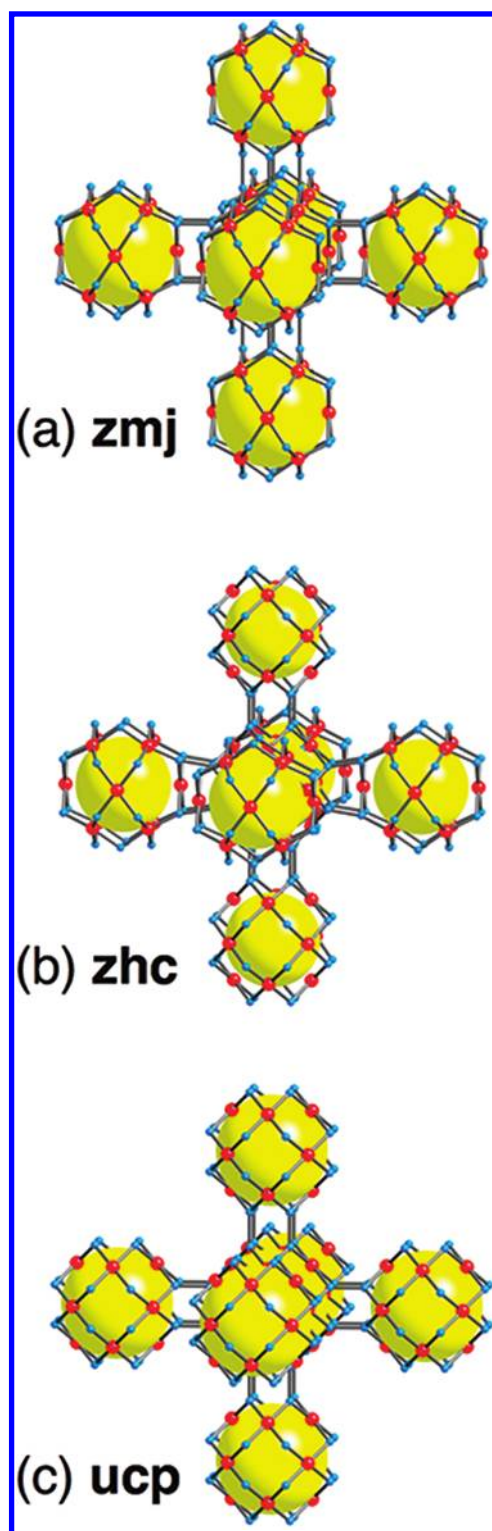


**Figure 41.** (a) The (3,4)-c net of the MOF in Figure 40a. (b) The (3,4)-c net of the MOF in Figure 40b. (c) The simplest binodal (3,4)-c net of this type.

AB and two BB links. The corresponding (4,5)-c net, **zhc**, has eight different kind of vertex. These two nets are illustrated in Figure 41. Clearly, there is a multitude of possibilities. The simplest, **ucp**, derived from all AA links between MOPs is a binodal (3,4)-c net. It is also shown in the figure. We have not yet found it in a MOF.

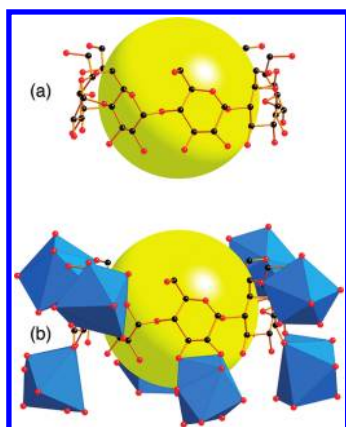


**Figure 42.** (a) A cyclodextrin unit from the CD-MOF. (b) The same with linked  $\text{KO}_8$  polyhedra.

### 5.6. A Cyclodextrin MOF

Here we discuss a MOF formed by coordination of alkali metal ions by  $\gamma$ -cyclodextrin (CD), a symmetrical cyclic oligosaccharide consisting of a ring of eight  $\text{C}_6$  monosaccharide units that is readily available in large quantities.<sup>75</sup> The resulting material (CD-MOF) which is built of enantiopure chiral organic components forms a cubic structure with chiral symmetry  $I432$ . We see though that the underlying net is achiral, symmetry  $Im\bar{3}m$ .

Figure 42 shows a cyclodextrin unit from the crystal structure, first alone and then with neighboring  $\text{KO}_8$  polyhedra. Each K is connected to four different rings and so is a 4-c vertex of the underlying net. Each cyclodextrin ring consists of eight  $\text{C}_5\text{O}$  rings, and the centers of these, which are of two kinds, are identified as 3-c vertices, as shown in Figure 43. A fragment of the (3,4)-c nets **rra** is shown in Figure 44. It may be seen that six eight-membered cyclodextrin rings (3-c green and magenta vertices) are linked by 4-c vertices (large blue balls) around a large central cavity. These are joined in turn in a body-centered cubic array.<sup>75</sup>

Further details of the analysis of this structure are provided in the Supporting Information.

### 5.7. The Hierarchical Underlying Nets of MIL-101 and MIL-100

MIL-101 is a complex MOF built from two simple components that are the trigonal prismatic basic chromium acetate SBU (Figure 7) and the ditopic terephthalate linker.<sup>76</sup> As may be seen from the fragment of the structure shown in Figure 45, the centers of the metal cluster SBUs are linked into corner-sharing tetrahedra to form a 6-c net. It is straightforward to identify all the crystallographically distinct SBUs (there are four) and to identify their neighbors. It will then be found that the net has the RCSR symbol **mtn-e**. This is a quadrinodal 6-c net (transitivity 4795) that at first sight seems surprisingly complicated to serve as the net of a MOF formed from two simple components. However, it turns out that the geometric requirement of linking  $\text{TX}_4$  tetrahedra with  $\text{T-X-T}$  angles of  $180^\circ$  and with eclipsed conformation as shown in Figure 41 leads inexorably to **mtn-e** as the optimum structure, a very nice example of how a simple local geometric restriction can lead to a complex periodic structure.<sup>77</sup> Note that the eclipsed conformation is a natural consequence of the trigonal-prismatic shape of the SBU; an octahedral SBU would lead to staggered tetrahedra.<sup>77</sup>

If we consider the points of extension of the metal cluster SBUs in MIL-101 as vertices, then we have a 4-c net of linked trigonal prisms with symbol **mtn-e-a**. Aspects of this net are

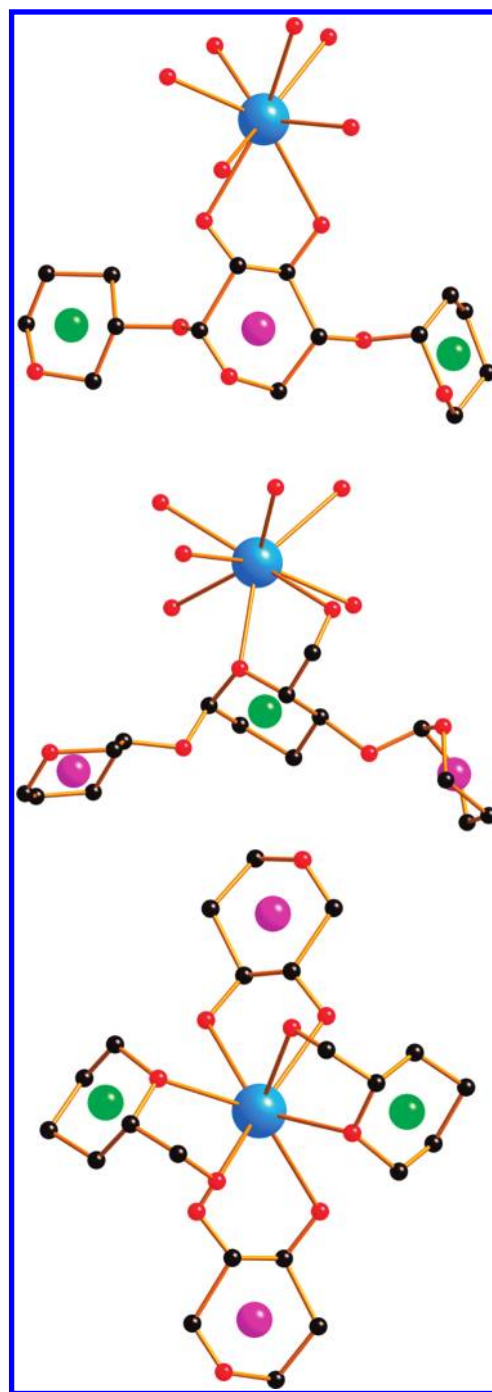


**Figure 43.** The three topologically distinct vertices in the CD-MOF shown as large spheres. The magenta and green are 3-c and the blue (metal atom site) is 4-c.

shown in Figure 46. It is the net of a simple tiling by trigonal prisms, truncated tetrahedra, and two large polyhedra. The smaller of these last is the Archimedean polyhedron, known as the truncated icosidodecahedron, which has 120 vertices with vertex symbol 4.6.10. The other polyhedron is larger and has two kinds of vertex, 120 with symbol 4.6.10 and 48 with symbol 4.6.12.

It is of interest to consider progenitors of the net. They are structures that should be in every chemistry textbook, but unfortunately, as of yet, generally they are not.

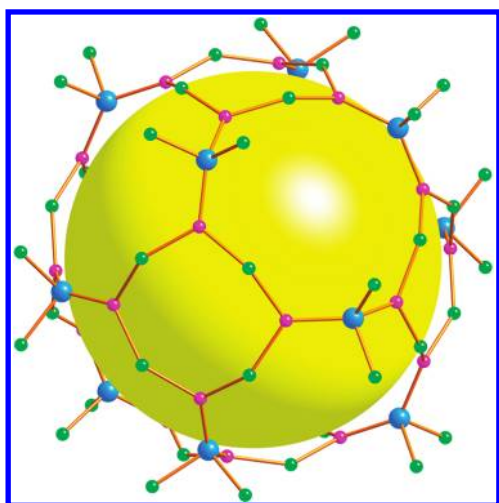


**Figure 44.** A fragment of the net (*rra*) of CD MOF. The eight-rings of alternating green and magenta nodes correspond to the cyclodextrin ring.

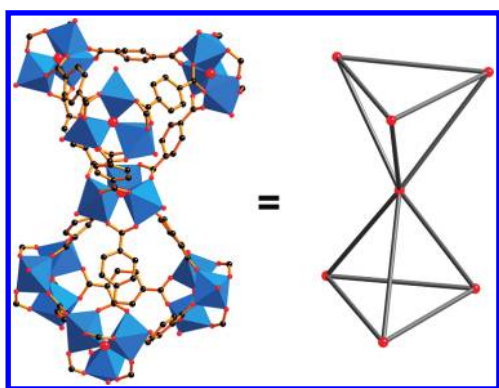


**Figure 45.** The corner-sharing tetrahedra in MIL-101. The corners are at the center of the basic chromium acetate SBU of Figure 7. The linkers are terephthalate.

The most common binary crystal structure in chemistry is named for  $\text{MgCu}_2$ . In this structure a diamond (*dia*) net of Mg is intergrown with a diamond edge net (*dia-e = crs*) of Cu. Taking just the nearest neighbors as edges, the new structure is a (6,12)-c net symbolized as *mgc*. However, it is clear that to correctly describe the structure and bonding in such structures we should consider next-nearest neighbors bonds and describe the structure as (12,16)-c. This extended structure has symbol *mgc-x*. A characteristic of intermetallic structures of this sort is that the atoms and links divide space into tetrahedra, as shown for *mgc-x* in Figure 47. The *dual* of this structure is obtained by putting new vertices in the centers of the tetrahedra and linking them by new edges to new vertices in adjacent tetrahedra. The dual structure will have RCSR symbol *mgc-x-d*, but in fact, it is “important” enough to deserve a new symbol, *mtn*. This new structure is a simple tiling and thus carries a 4-c net, which is the net of the zeolite with framework code MTN. The same structure is known as type II clathrate hydrate structure. Thus, to trace the genesis of the MIL-101 structure, we could label the augmented net *mgc-x-d-e-a* (but please do not).

A related MOF from the same group is known as MIL-100.<sup>78</sup> In this the same metal cluster, SBUs are joined by the tritopic linker trimesate (benzene-1,3,5-tricarboxylate). Again the structure

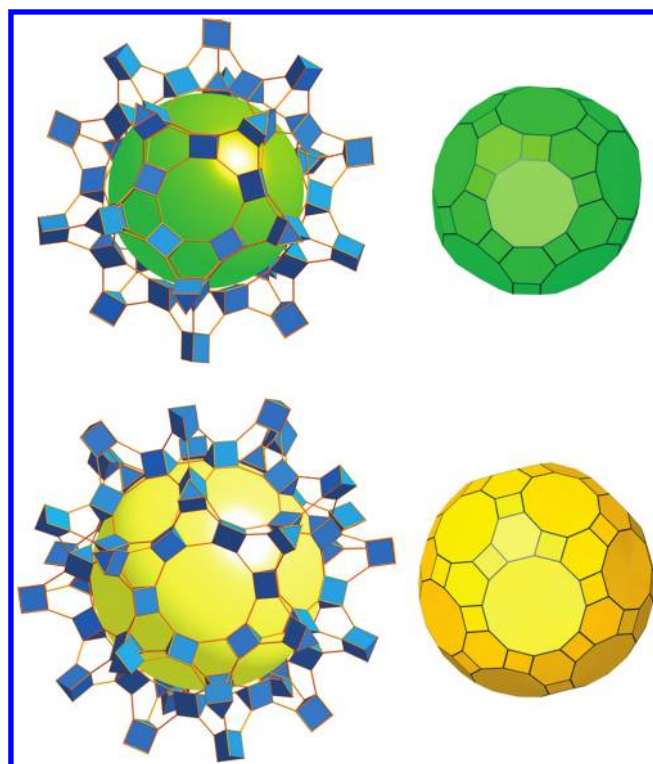


**Figure 46.** The cavities in the augmented net of MIL-101. The net is *mtn-e-a*.

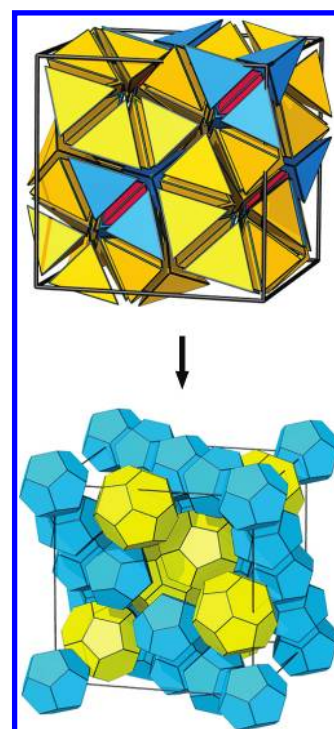


**Figure 47.** Generation of the tiling of the net *mtn* (bottom) as the dual of the tiling of the net *mgc-e* (top).

is based on corner-sharing tetrahedra in eclipsed conformation, and a related structure is obtained. Now though there are 3-c vertices in the net corresponding to the center of the trimesate

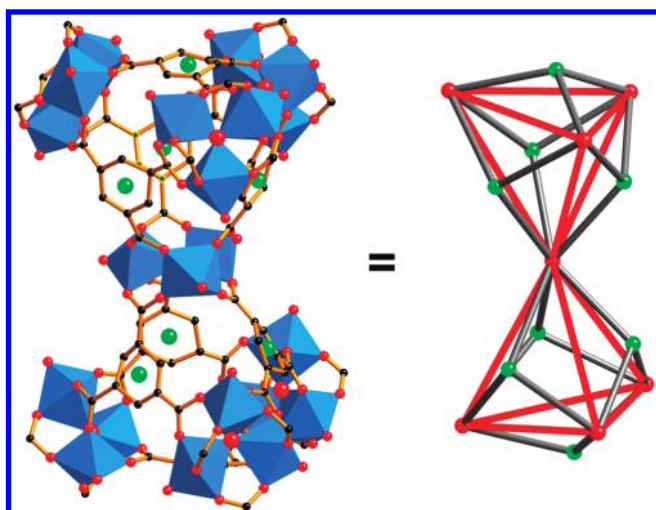


**Figure 48.** A fragment of the structure of MIL-100. Green balls are 3-c nodes of the underlying net (**moo**). 6-c nodes are at the center of the blue SBU. On the right, the red lines outline the tetrahedra.

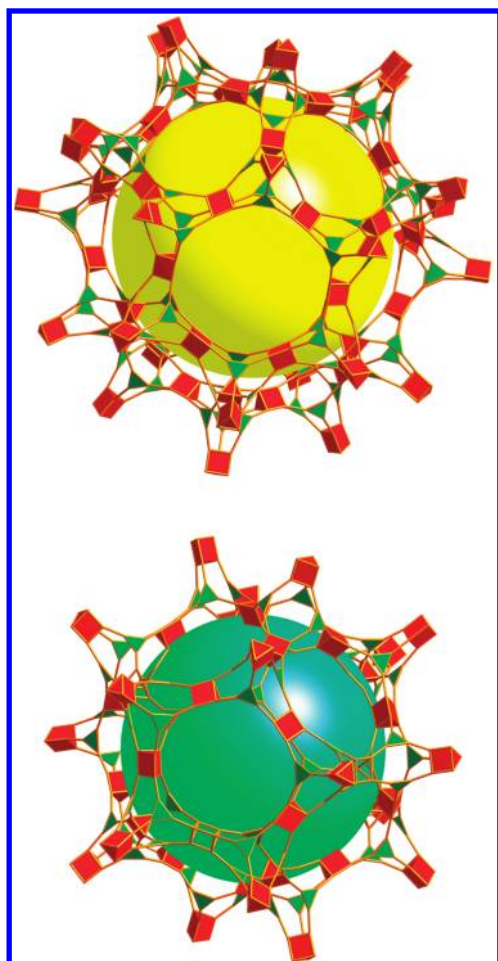


**Figure 49.** Fragments of the net **moo-a** as linked triangles and trigonal prisms and showing the two large cavities (yellow and green balls).

six-membered ring and a (3,6) net, the RCSR symbol **moo** is generated (Figure 48). Fragments of the corresponding augmented net of linked triangles and trigonal prisms are shown in Figure 49.

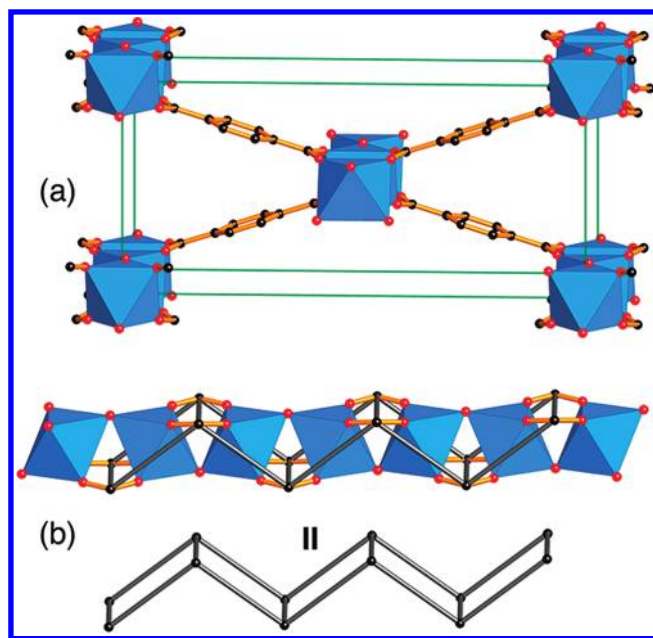


**Figure 50.** Aspects of the structure of MOF-71. (a) View along the rod direction showing how the rods are linked. (b) One rod with the points of extension (carboxylate C atoms) linked into a zigzag ladder.

A spectacular isorecticular material meso-MOF-1 with Tb in the trigonal prismatic SBU and triazine-1,3,5-tribenzoate as linker has since been reported.<sup>79</sup> This material has a face-centered cubic unit cell edge of 123.9 Å and cage diameters of 3.9 and 4.7 nm. Note that in all these materials the arrangement of the two large cages is that of Mg and Cu in MgCu<sub>2</sub>.

## 6. MOFS WITH ROD SBUS

Rod MOFs contain infinite 1-periodic SBUs (rods).<sup>80</sup> They are of interest as they usually have parallel channels and often exhibit pronounced “breathing”, in which the rods act as hinges.<sup>81</sup> Recall that for finite metal-containing SBUs we generally could identify  $k$  points of extension that defined a polygon or polyhedron with  $k$  vertices in the center of which we recognize a  $k$ -c vertex of a net. Such a procedure is hard to adapt to rod SBUs. In some instances, we can associate the points of extension with a rodlike structure, such as a ladder, but in other instances, the reduction to a net is a little more arbitrary and we then proceed on an ad hoc basis, but treating the organic linkers in the same way as before. The difficulty is even more pronounced for MOFs in which metal atoms sharing points of extension are in continuous two-periodic layers; these occur rather rarely.

### 6.1. SBUs as Zigzag Ladders

A versatile and often-studied group of MOF structures is variously known as MIL-47/MIL-53/MIL-60<sup>82</sup> and MOF-71.<sup>80</sup> The metal SBU consists of a rod of MO<sub>6</sub> octahedra sharing opposite corners and with stoichiometry MX(CO<sub>2</sub>)<sub>2</sub>, X = O or OH and M = Al, Cr, Co, Fe, Ga, or V. Figure 50 illustrates MOF-71, basic vanadium terephthalate with framework VO(bdc)<sub>2</sub> (bdc = benzene-1,4-dicarboxylate). The figure also depicts one rod showing that the points of extension (the carboxylate C atoms) fall on a zigzag ladder (often called a “double zig-zag”).

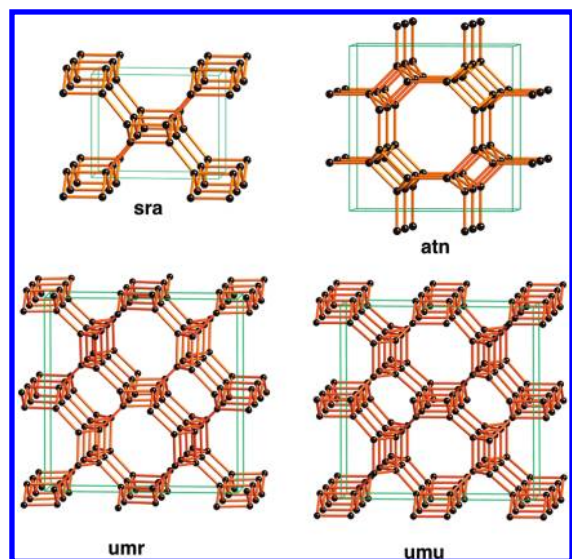


Figure 51. Four ways of linking zigzag ladders into uninodal 4-c nets.

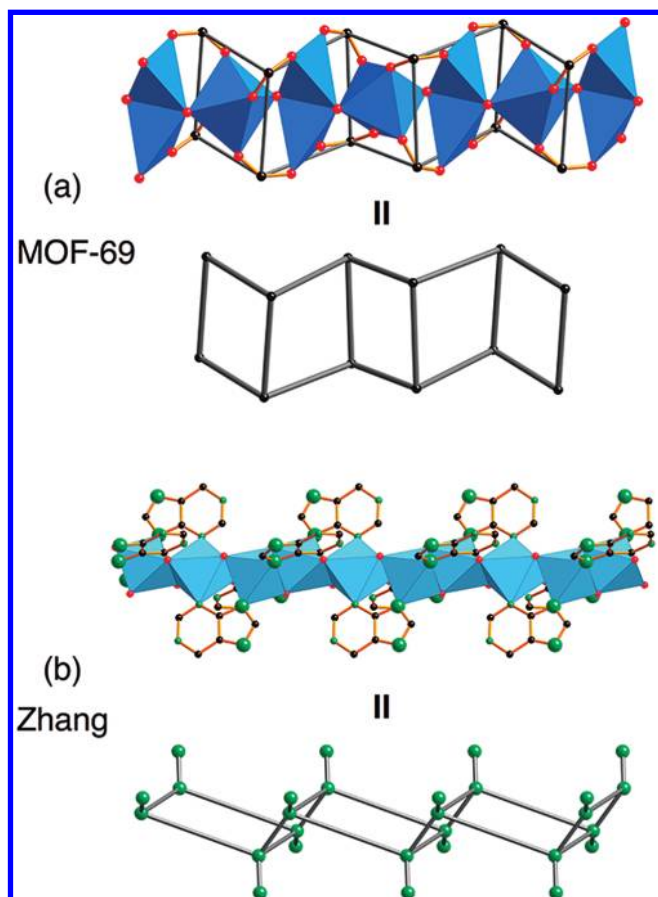


Figure 52. Two rods with points of extension forming a zigzag ladder. (a) In MOF-69, the points of extension are carboxylate C atoms and (b) a rod SBU reported by Zhang et al.<sup>80</sup> The linker has three N atoms (green) but only two (larger spheres) are considered as nodes of the underlying net.

These are linked by ditopic linkers to form the uninodal 4-c net **sra** illustrated in Figure 51.

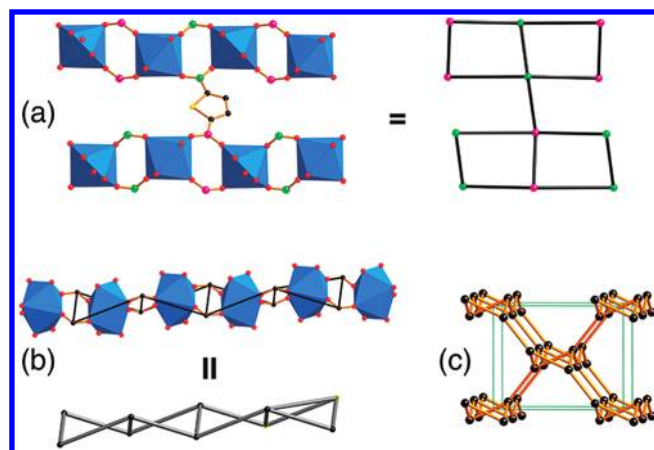


Figure 53. Aspects of the structure of MOF-75. (a) Two rod SBUs connected by a linker (yellow sphere is an S atom). The carboxylate C atoms forming the points of extension are of two crystallographic kinds in the crystal. These are shown as magenta and green on the fragment of the net on the right. (b) Left: one rod showing that the points of extension form a twisted ladder. Right: the underlying net **irl**.

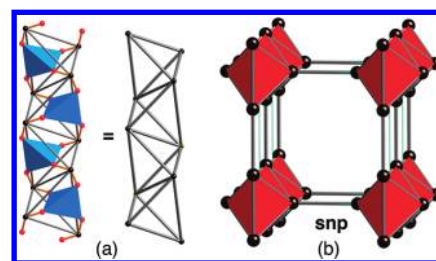


Figure 54. (a) The structure of the points of extension of the MOF in Figure 20 interpreted as a rod of edge-sharing tetrahedra. (b) The net of these rods linked by ditopic linkers.

Another MOF with the same underlying net is MOF-69.<sup>83</sup> The rods now consist of metal–oxygen octahedra and tetrahedra, as shown in Figure 52, but the points of extension again form zigzag ladders linked as in **sra**.

Yet another rodlike SBU with points of extension forming zigzag ladders is also shown in Figure 52.<sup>84</sup> In this last case, links between the ladders are via the imidazole ring part of hypoxanthine, and as the authors noted, the ladders are now linked in a different way, that of the net **umr** (Figure 51). This net and two other uninodal ways (**atn** and **umu**) of linking zigzag ladders (Figure 51) were overlooked in our earlier account of uninodal nets for linking rodlike SBUs.<sup>80</sup> Although at first glance **umr** and **umu** look very similar, they actually have different symmetries ( $I4_1/acd$  and  $I4_1/amd$ , respectively).

## 6.2. A MOF with a Twisted Ladder Rod SBU

In MOF-75, rods of linked  $TbO_8$  dodecahedra are linked by the ditopic linker 2,5-thiophene dicarboxylate.<sup>80</sup> Figure 53a shows two rods and one linker. In the crystal there are two kinds of carboxylate carbons, the points of extension. These form a ladder along the rod, as shown in the figure. Figure 53b shows that the ladder is now twisted compared to the zigzag ladders of the previous sections. When the connectivity of the two vertices is submitted to Systre, it is found that topologically the net is the uninodal **irl** illustrated in Figure 53c. Other uninodal ways of linking twisted ladders are **uoa** and **uoe** (see the RCSR database).

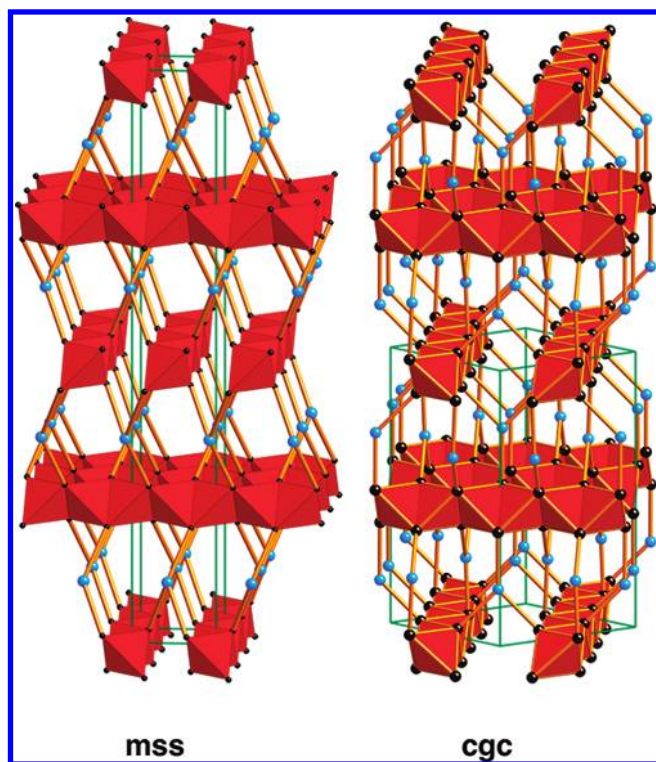


Figure 55. Two nets formed by linking rods of edge-sharing tetrahedra.



Figure 56. A tritopic pyrazole-based linker with a 3-c vertex shown in magenta. The large black spheres are the C atom points of extension of rod SBUs.

### 6.3. A MOF with Rod SBUs of Linked Tetrahedra

We remarked in section 4.5 that the MOF (Figure 20) whose topology had been described as **pts** was better considered as a rod MOF with the rods linked by ditopic linkers. Figure 54 displays one rod of the structure showing that the points of extension (carboxylate carbons) form a rod of tetrahedra sharing opposite edges. Linking these by edges corresponding to the ditopic linkers produces the uninodal 6-c net **snp**, also shown in the figure.

### 6.4. Two-Way Rod SBUs of Linked Tetrahedra

In MOF-77<sup>80</sup> the rod SBUs consist of  $\text{ZnO}_4$  tetrahedra linked by carboxylates, and the points of extension form a rod of edge-sharing tetrahedra in exactly the same way as shown in Figure 54. The organic linker is the tetratopic 1,3,5,7-adamantanetetracarboxylate (see Figure 10), the center of which is a 4-c vertex of the underlying net. The other vertices of the net are the carboxylates

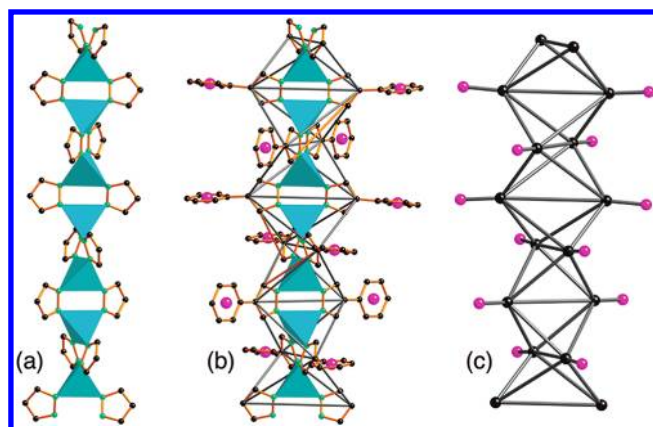


Figure 57. (a) A rod of linked  $\text{ZnN}_4$  tetrahedra. (b) The same showing the mode of linking to the linker of Figure 56. (c) The nodes of the underlying net.

which are joined to five other carboxylates and to the 4-c vertex to form the (4,6)-c net **mss** shown in Figure 55.

A variation on this theme is a MOF containing rods of linked  $\text{ZnN}_4$  tetrahedra joined by a tritopic pyrazole-based linker shown in Figure 56.<sup>85</sup> In the figure, a 3-c node of the underlying net is shown as magenta and C atom points of extension of the rod are shown as larger black spheres. Again the points of extension form rods of edge-sharing tetrahedra, as shown in Figure 57. These are linked now by 3-c vertices to form the (3,6)-c net **cgc** shown in Figure 53.

These structures provide rare examples of rod MOFs with rod axes in two different directions. Note that in the first structure the rods form a four-layer sequence along the axis normal to those of the rods. In the second case, it is a two-layer sequence. These are respectively patterns 5 and 6 in our review of rod packings in MOFs.<sup>80</sup>

### 6.5. MOFs with Rod SBUs of Linked Octahedra

A structure discussed by Alexandrov et al.<sup>26</sup> (identified by them as CDC code AFOYOK) consists of  $\text{CuN}_6$  octahedra linked by triazole/tetrazole linkers.<sup>64</sup> A rod from the structure is shown in Figure 58. The net was identified as a binodal (4,6)-c net with vertices corresponding to the Cu atoms, and the center of the linkers are considered as tetratopic. However, as discussed in a similar case in section 6.3, we consider the Cu octahedra to share points of extension with their neighbors and thus form an infinite rod SBU. The points of extension are the C atoms of the five-membered rings that are shown as larger spheres in the figure. These points of extension form a rod of octahedra linked by sharing opposite faces as also shown in the figure. Finally, linking these rods produces the binodal 7-c net **oab** also illustrated in the figure.

A related structure is found in  $\text{Sc}(\text{bdc})_3$  ( $\text{bdc}$  = 1,4-benzenedicarboxylate = terephthalate) with Sc in octahedral coordination.<sup>87</sup> Again, there are rods of octahedra now sharing carboxylate C atoms as points of extension, and these points of extension form rods of face-sharing octahedra (Figure 59). The linking of these rods gives the binodal 7-c net **sct** (Figure 60). There is a closely related uninodal 7-c net **wnf** again constructed by linking rods of face-sharing octahedra (Figure 60), and it is natural to ask why the lower-symmetry ( $Fddd$ ) binodal topology is adopted rather than the more symmetrical ( $R\bar{3}m$ ) uninodal one. The answer appears to be that the latter has two kinds of octahedron; compare just one

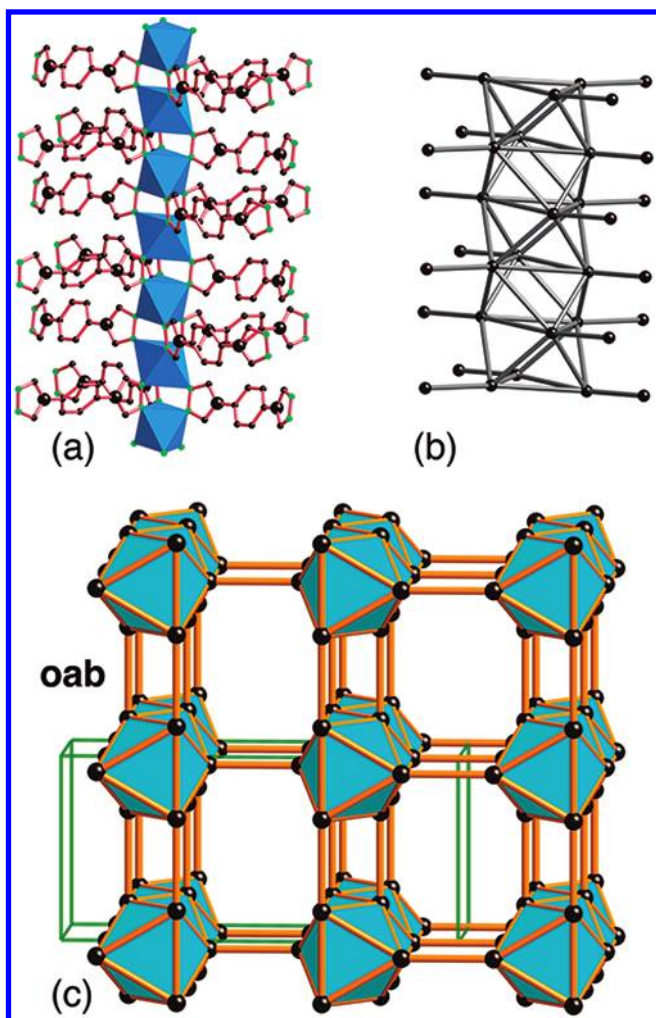


**Figure 58.** (a) A rod of  $\text{CuN}_6$  octahedra (N atoms green) linked by ditopic linkers. The points of extension are C atoms shown as large black spheres. (b) The SBU of face-sharing octahedra formed by these points of extension. (c) The underlying 7-c net **oab**.

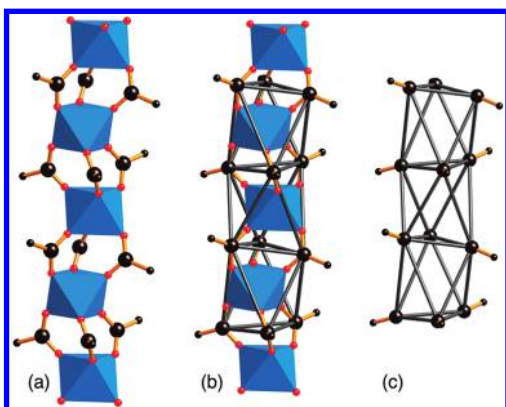


**Figure 59.** A rod in the structure of  $\text{Sc}(\text{bdc})_3$ . (a) A rod with carboxylate C atoms (points of extension) as large black spheres. (b) The same with points of extension linked by edges. (c) Just the linked points of extension.

kind in the former. Applied to the real structure the chosen structure is that with just one kind of Sc atom (Sc atoms center the octahedra of the underlying net).

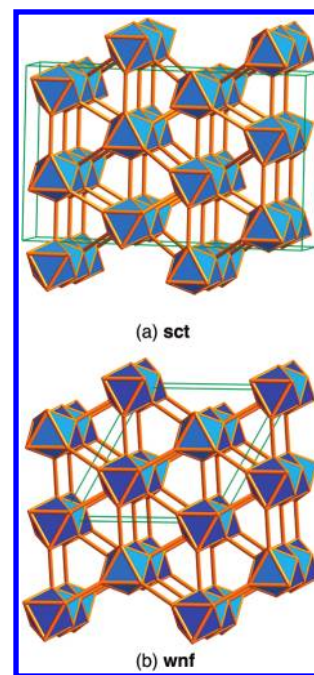


**Figure 60.** Two ways of linking rods of face-sharing octahedra. (a) The binodal net **sct** that is the underlying net of  $\text{Sc}(\text{bdc})_3$ . (b) The uninodal net **wnf**. This net has two kinds of octahedra, shown as dark and light blue.

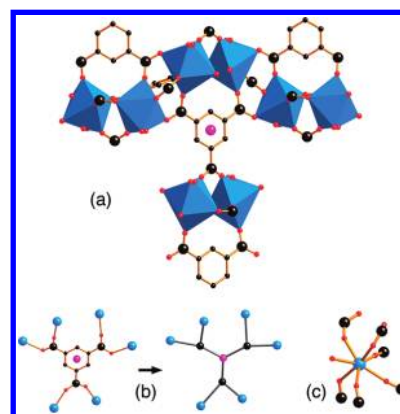


**Figure 61.** (a) A fragment of the structure of MOF-76. The magenta ball marks a 3-c vertex linked to carboxylate C atoms (large black ball). (b) Showing the 3-c vertices of the underlying net. (c) Showing that the blue vertices are 6-c.

An interesting alternative deconstruction of the  $\text{Sc}(\text{bdc})_3$  structure has also been suggested.<sup>88</sup> In this approach, vertices are placed in the centers of the octahedron faces normal to the rod axis. These vertices are linked to three others on adjacent rods and to two on the same rod) one above and one below). One then gets the uninodal 5-c net **ghw**. This is an attractive simplification, but it obscures the shape of the rod SBU.

### 6.6. Rod SBUs That Resist Simplification

Not all rod SBUs have points of extension that form a simple envelope such as a ladder or rods of linked polyhedra in the previous examples. For these it seems that the best strategy for describing the topology is to include the individual metal atoms

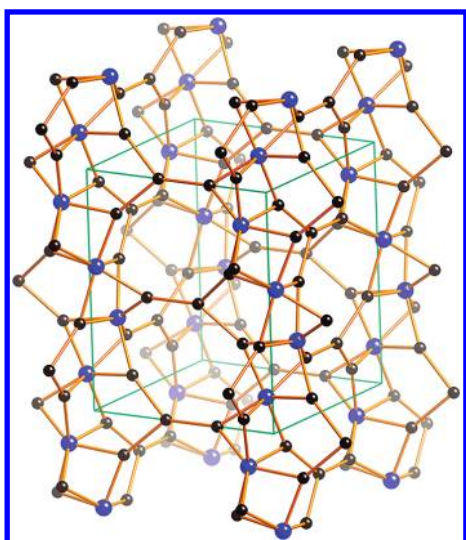


Figure 62. The net **rnb** of MOF-76. Blue vertices are the 6-c vertices.

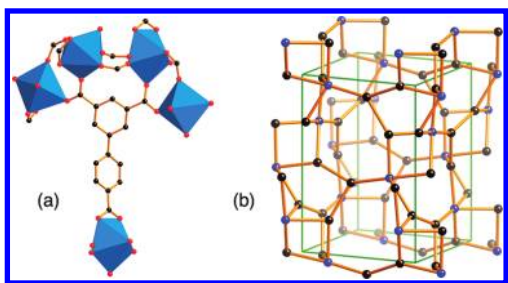


Figure 63. (a) A fragment of a rod net reported by Guo et al.<sup>90</sup> This is deconstructed in the same way as MOF-76 (see Figure 61). (b) The underlying (3,6)-c net **rnc** (compare Figure 62).

as vertices. Note that this is not what we have done for any of the finite-cluster metal-containing SBUs in any of the above examples. To illustrate this point, we use the structure of MOF-76,<sup>80</sup> one which has attracted some subsequent attention.<sup>89</sup> In this material,  $\text{TbO}_7$  polyhedra are joined by carboxylate links into rods with a rather irregular array of points of extension. The carboxylate linker is the tritopic 1,3,5-benzenetricarboxylate. A fragment of the structure is shown in Figure 61. As shown in the figure, we take the center of the organic linker to be a 3-c vertex linked to three carboxylate C vertices that are in turn linked also to two metal atoms, so these are also 3-c vertices. Notice that these are of two different kinds. Finally, the metal atoms are linked to six carboxylate vertices, so the net is (3,6)-c. This net, which is intrinsically chiral (space group  $P4_322$ ), has RCSR symbol **rnb** and is illustrated in Figure 62. It is rather complex, but one must sometimes just take what one gets.

A recently published related chiral rod structure again with atoms joined by a tricarboxylate linker has some similarities, but reference to Figure 63 shows an additional complication.<sup>90</sup> Two of the carboxylates are joined to two different metal atoms, and the C atoms are considered as branch points; however, the third carboxylate is linked to just one metal atom, so there is not an associated branch point. Again, the net (Figure 63) is rather complicated for such simple components and has low symmetry ( $P4_3$ ). It is assigned the RCSR code **rnc**.

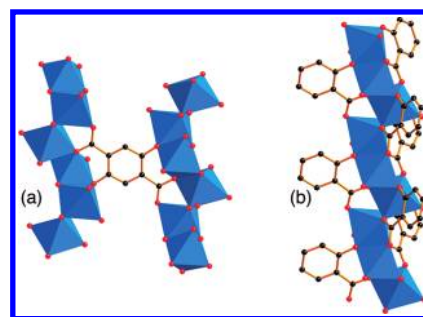


Figure 64. Fragments of the structure of MOF-74. (a) One linker joining two rods. (b) The pattern of linkers from one rod.

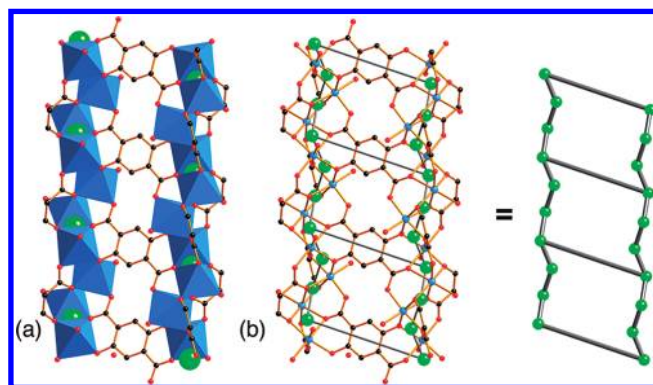


Figure 65. Deconstruction of MOF-74. Each end of the linker is joined to four metal-atom polyhedra replaced by a large green ball. These are shown (a) only for the linkers shown (which are in the plane of the drawing). (b) All the green balls, which are 3-c vertices, are shown.

A final example of a rod SBU is that found in MOF-74,<sup>80</sup> a structure that has attracted some attention recently as the magnesium analog.<sup>91</sup> In this material, rods of edge-sharing  $\text{ZnO}_6$  octahedra are joined by 2,5-dihydroxy-1,4-benzenedicarboxylic acid, as shown in Figure 64. Each rod, which taken alone is chiral, is linked to three others of opposite hand. The rod is very condensed; each linker joins four octahedra on one rod to four on another. Each carboxylate is linked to three Zn octahedra, and the hydroxy O is linked to two Zn octahedra. Identifying all the branching points would result in a net of such complexity that it would lead to little insight into the underlying topology.

A possible strategy is to replace the linker by an 8-c vertex linked to four metal atoms on each rod. The metal atoms in turn serve as 4-c vertices, and a (4,8)-c net results. This is, in fact, the solution adopted by Alexandrov et al.<sup>36</sup> However, we do not adopt this approach; the net does not contain any links along the rod itself, and it is hard to justify finding a point on the linker as an 8-c vertex.

Accordingly, in this case we resort to the simplification shown in Figure 65. In the simplified net, vertices are placed in the center of the group of four octahedra linked by each linker (large green balls in the figure), and a single edge links these vertices to one on an adjacent rod. In a way, we have broken the rod into a sequence of subunits lined along the rod. The resulting net (Figure 66) is the uninodal 3-c net with symbol **etb**, one of the two ways of linking 3-fold helices, which now represent the rod SBUs, into uninodal nets (the other possibility is **eta**).<sup>80</sup>

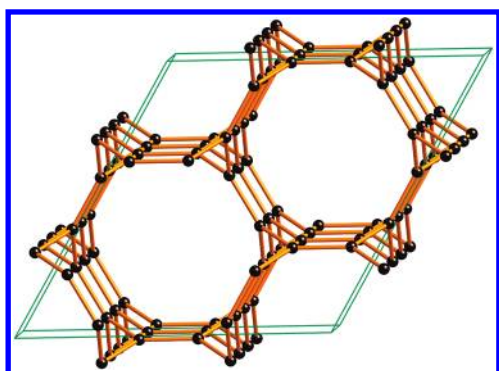


Figure 66. The 3-c net **etb**. Each helix is bonded to others of opposite hand.

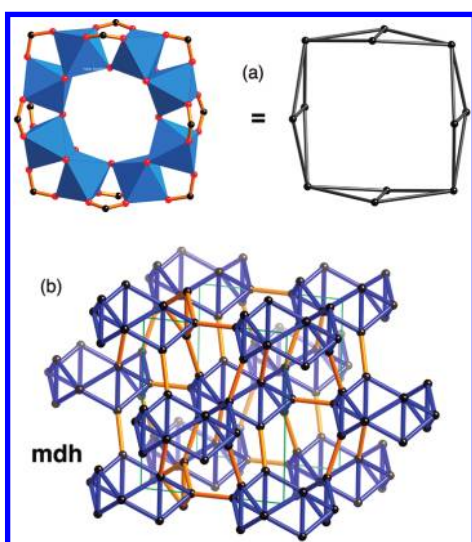


Figure 67. (a) ring SBU of eight  $\text{TiO}_6$  octahedra and the pattern of the points of extension. (b) The (5,4)-c net obtained by linking each SBU to 12 neighbors.

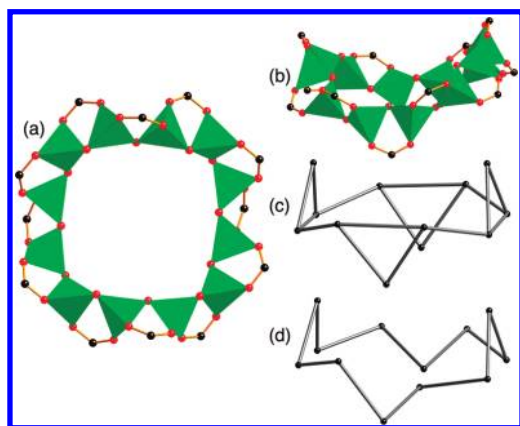


Figure 68. (a and b) An SBU formed of 12  $\text{BeO}_4$  tetrahedra. (c and d) Two ways of linking the points of extension.

## 7. MOFS WITH RING SBUS

MOFs with cation coordination polyhedra that form rings are so far relatively rare. Here we consider just two examples from the recent literature.

The first example is a basic titanium terephthalate, in which eight  $\text{TiO}_6$  octahedra are joined in a ring by edge and vertex sharing, and

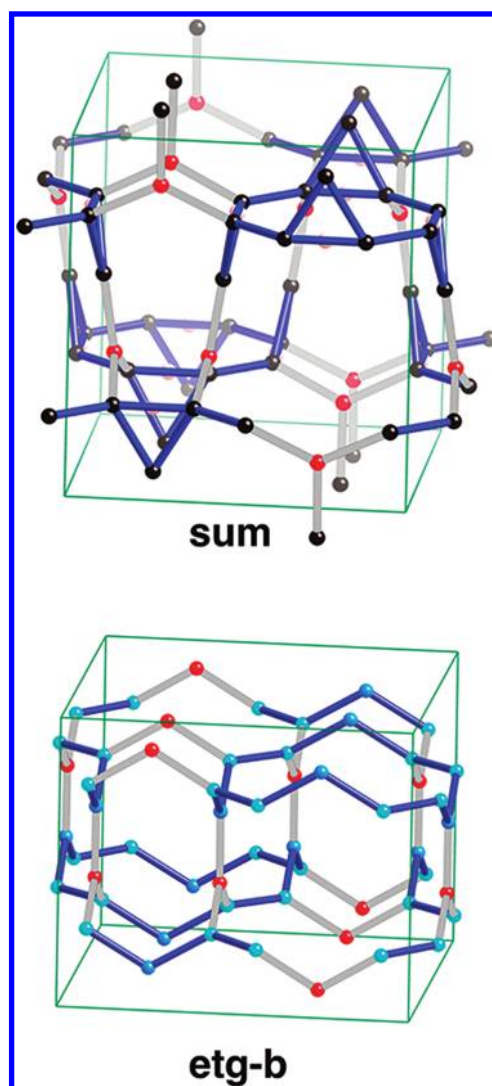


Figure 69. Two nets formed by linking the 12-ring SBU corresponding to the two ways of linking the points of extension in Figure 68 (see the text).

the rings are linked by terephthalate.<sup>92</sup> Each ring has 12 points of extension, as shown in Figure 67, and is linked to 12 others by the terephthalate linkers to form a (4,5) binodal net **mdh**.

The topology of the linkage between rings is the 12-c net **fcu** of the face-centered cubic lattice, and one might consider the net as an augmented form of **fcu**, as the authors suggest. However, the ring SBU has a very different shape from a cuboctahedron, which is the most regular vertex figure of **fcu**, so we prefer to consider the topology as described by the new net **mdh**.

Our final example is a MOF with rings of 12  $\text{BeO}_4$  tetrahedra linked by corner-sharing reported by Sumida et al.<sup>93</sup> The points of extension are carboxylate C atoms of 1,3,5-benzenetribenzoate. The 12 points of extension form a puckered ring with 2-c and 3-c vertices, as shown in Figure 68. Combining these with the 3-c vertices of the linker gives the (3,4)-c net **sum** with symmetry  $P4_2/nmc$  illustrated in Figure 69.

### 7.1. Coda

Readers who have read through this long paper deserve a finishing treat, and here it is, at least for those who love nets: If we instead considered the points of extension of the Be SBU in the previous paragraph as forming a ring of all 2-c vertices, as shown in Figure 68, then the net obtained by combining with the

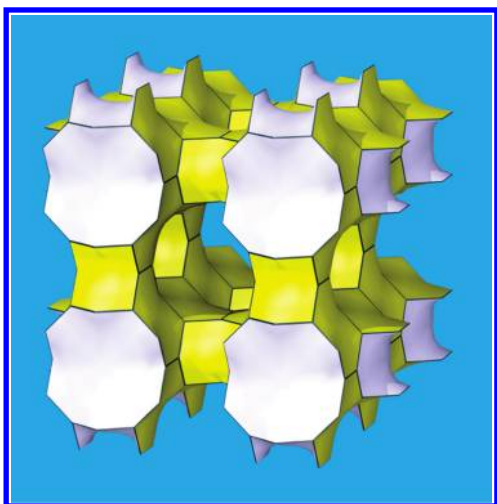


Figure 70. The net **etg** as an  $8^3$  tiling of the *CLP* minimal surface.

organic linker vertices will be 3-c. The vertices of the ring are of two kinds: A vertices at the acute angles and B vertices at obtuse angles. To form the net these combine with linker vertices (C) in the ratio  $2A + B + C$ . However, it turns out that vertices B and C are topologically equivalent, so Systre tells us that the net is the binodal 3-c net **etg** with symmetry  $P4_2/mcm$ . To distinguish between B and C vertices, we have to go to a subgroup, which with knowledge of the symmetry of **sum** (previous paragraph) we identify as the  $k$  subgroup  $P4_2/nmc$  with  $a' = \sqrt{2}a$  (this would have been hard to find without the help from Systre). It is, in fact, common for topologically equivalent vertices of nets to correspond to different chemical species. For example, in NaCl the Na and Cl atoms are at the vertices of the 6-c net **pcu**. If we want to distinguish the chemical types of vertices, we have to go to lower symmetry. Such lower symmetry (binary or black-and-white) nets are distinguished by an extension **-b** in RCSR and are reported there with the lower symmetry. The net **etg-b** is illustrated in Figure 69 with the 12-rings emphasized.

There is more to the net **etg**. The vertex symbol for both vertices is 8.8.8. The lack of subscripts tells us that the net is that of a tiling of a periodic surface and is derived from the regular hyperbolic tiling  $\{8,3\}$  (please note that this is a *real* Schläfli symbol) and the symmetry leads us to expect that the tiling is of the genus 3 minimal surface *CLP*. This is indeed the case and the net is illustrated this way in Figure 70.

## 8. CONCLUDING REMARKS

In this review we have indicated how we reduce a complex crystal structure to an underlying topology. We emphasize that it is not a review of MOF structures. Indeed, we have ignored many of the most interesting and potentially useful materials as they consist of finite SBUs with well-defined geometric shapes that are joined by simple ditopic or tritopic linkers; in these instances, identifying the underlying net is trivial (with the help of Systre). Likewise, our selection of examples is not systematic.

Our approach to identify vertices of underlying nets may be summarized as follows:

- (A) Metal cluster SBUs consisting of metal atoms sharing points of extension.
  - (i) If finite, identify the envelope as a polygon or polyhedron with the  $k$  points of extension as vertices. The SBU can usually be reduced to a  $k$ -c vertex, but if this

results in a higher symmetry net, it is preferable to keep the points of extension as vertices.

- (ii) For rods or rings, identify if possible the envelope of points of extension (e.g., as a ladder). No further simplification is possible.
- (B) Organic, or mainly organic, SBUs. These are, so far, finite. Use all branching points of the molecular fragment as vertices.

We have indicated in several places that we differ in some details with the approach described by Alexandrov et al.<sup>36</sup> However, we do not take issue with their main results about the frequency of occurrence of the more-important nets, and we note that the results of all the analyses are available as very valuable Supporting Information for that paper. As already remarked, the great majority of MOFs have just one “obvious” underlying net. For the less obvious ones, it is important to analyze the nodes and edges of structure manually and the data to be submitted to Systre. We have indicated in several places how this is done. Then one can compare the results from computer assistance provided by TOPOS. We hope disagreements will be fairly rare.

We have remarked that the process of deconstruction is rather like reverse engineering. The reason for undertaking reverse engineering of something is to find out how it is made and then to apply that knowledge to make better things. It is in this spirit, as a guide to designed synthesis of new materials, that this paper is offered. We hope also that we have indicated that some knowledge of graph theory and space groups is a valuable component of the MOF chemist’s toolbox.

We have said nothing about the many examples of structures in which two or more copies of a net occur independently (in the graph-theoretic sense) in interpenetrating structures. There appears to be no satisfactory topological theory of such structures as yet. When it appears it might be expected to have some flavor of, yet be quite distinct from, knot theory.<sup>94</sup> We await it eagerly.

## ASSOCIATED CONTENT

### Supporting Information

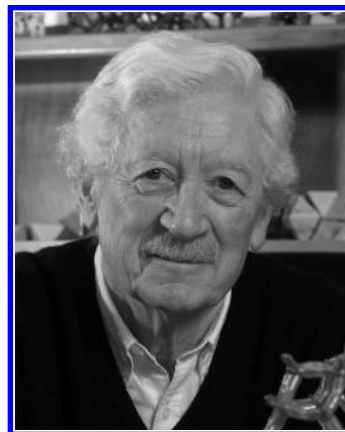
Deconstruction of the CD-MOF. This material is available free of charge via the Internet at <http://pubs.acs.org>.

## AUTHOR INFORMATION

### Corresponding Author

\*E-mail [mokeeffe@asu.edu](mailto:mokeeffe@asu.edu) (M.O.), [yaghi@chem.ucla.edu](mailto:yaghi@chem.ucla.edu) (O.M.Y.).

## BIOGRAPHIES



Michael O'Keeffe was born in Bury St Edmunds, England in 1934. He attended the University of Bristol (B.S. in 1954, Ph.D. in 1958, and D.Sc. in 1976). He is Regents' Professor of Chemistry at Arizona State University, where he has been since 1963. Past research has included investigations of conductivity, diffusion, defects, and nonstoichiometry in solids and experimental and theoretical studies of crystal chemistry. Over the last dozen years he has collaborated with Prof. Yaghi, his coauthor on this paper, in applying the theory of periodic structures to the development of the theoretical basis of designed synthesis of materials, such as MOFs, consisting of linked molecular fragments of predetermined shapes (reticular chemistry).



Omar M. Yaghi was born in Amman, Jordan, in 1965. He received his Ph.D. from the University of Illinois—Urbana (1990) with Prof. Walter G. Klemperer. He was an NSF Postdoctoral Fellow at Harvard University (1990–92) with Professor Richard H. Holm. He has been on the faculties of Arizona State University (1992–98) and University of Michigan (1999–2006). His current position is the Irving and Jean Stone Professor in Physical Sciences, Professor of Chemistry and Biochemistry, and Molecular and Medical Pharmacology at UCLA and he also directs the Center for Reticular Chemistry. His work encompasses exploring the synthesis, structure, and properties of inorganic compounds and the design and construction of new crystalline materials. He has also pioneered a global mentoring model for building centers of excellence for scientific collaborations between the United States and other countries. The model is being implemented in centers established in a growing number of countries in Asia and the Middle East.

## ACKNOWLEDGMENT

M.O. acknowledges very detailed and useful discussions on deconstructing crystal structures with Vladislav Blatov, Charlotte Bonneau, and Davide Proserpio. Gérard Férey assisted with helpful correspondence and data for MIL-100 and MIL-101. M.O. also acknowledges support from the U.S. National Science Foundation, grant number DMR 0804828. O.M.Y. is supported by KAIST, WCU program.

## REFERENCES

- (1) O'Keeffe, M. *Chem. Soc. Rev.* **2009**, *38*, 1215.
- (2) (a) Farha, O. K.; Yazaydin, O. E.; Eriazici, I.; Malliakas, C. D.; Christos, D.; Hauser, B. G.; Kanatzidis, M. G.; Nguyen, S. T.; Snurr,

R. Q.; Hupp, J. T. *Nature Chem.* **2010**, *2*, 944. (b) Yazaydin, A. O.; Snurr, R. Q.; Park, T. H.; Koh, K.; Liu, J.; LeVan, M. D.; Bemin, A. I.; Jakubczak, P.; Lanuza, M.; Galloway, D. B.; Low, J. J.; Willis, R. R. *J. Am. Chem. Soc.* **2009**, *131*, 18198.

(3) see e.g. Ewald, P. P.; Hermann, C., Eds. *Strukturbericht 1913–1928*; Akademische Verlagsgesellschaft M. B. H.: Leipzig, 1931.

(4) (a) Wells, A. F. *Three-Dimensional Nets and Polyhedra*; Wiley: New York, 1977. (b) Wells, A. F. *Further Studies of Three-Dimensional Nets*; Monograph 9; Am. Cryst. Assoc.: Littleton, CO, 1979.

(5) (a) Iwamoto, T. *Inclusion Compounds*; Atwood, J. L., Davies, J. E. D., MacNicol, D. D., Eds.; Oxford Univ. Press: London, 1991; Chapter 6. (b) Kitazawa, T.; Nishikiori, S.; Iwamoto, T. *J. Chem. Soc. Dalton* **1994**, 3695. (c) Iwamoto, T.; Kitazawa, T.; Nishikiori, S.; Yuge, H. *J. Chem. Soc. Dalton* **1997**, 4127. These papers give references to the extensive earlier work of this group.

(6) (a) Hoskins, B. F.; Robson, R. *J. Am. Chem. Soc.* **1990**, *112*, 1546. (b) Robson, R. *J. Chem. Soc., Dalton Trans.* **2000**, 3735.

(7) Bowes, C. L.; Ozin, G. A. *Adv. Mater.* **1996**, *8*, 13.

(8) Schindler, M.; Hawthorne, F. C.; Baur, W. H. *Acta Crystallogr. B* **1999**, *55*, 811.

(9) O'Keeffe, M.; Eddaoudi, M.; Li, H.; Reineke, T. M.; Yaghi, O. M. *J. Solid State Chem.* **2000**, *152*, 3.

(10) (a) Yaghi, O. M.; O'Keeffe, M.; Ockwig, N. W.; Chae, H. K.; Eddaoudi, M.; Kim, J. *Nature* **2003**, *423*, 705. (b) Ohrstrom, L.; Larsson, K. *Molecular Based Materials: The Structural Network Approach*; Elsevier: Amsterdam, 2005.

(11) Ockwig, N. W.; Delgado-Friedrichs, O.; O'Keeffe, M.; Yaghi, O. M. *Acc. Chem. Res.* **2005**, *38*, 176.

(12) Eddaoudi, M.; Kim, J.; Rosi, N.; Vodak, D.; Wachter, J.; O'Keeffe, M.; Yaghi, O. M. *Science* **2002**, *295*, 469.

(13) (a) Delgado-Friedrichs, O.; O'Keeffe, M.; Yaghi, O. M. *Acta Crystallogr. A* **2003**, *59*, 22. (b) Delgado-Friedrichs, O.; O'Keeffe, M.; Yaghi, O. M. *Acta Crystallogr. A* **2003**, *59*, 515. (c) Bonneau, C.; Delgado-Friedrichs, O.; O'Keeffe, M.; Yaghi, O. M. *Acta Crystallogr. A* **2004**, *60*, 517. (d) Delgado-Friedrichs, O.; O'Keeffe, M.; Yaghi, O. M. *Acta Crystallogr. A* **2006**, *62*, 350. (e) Delgado-Friedrichs, O.; O'Keeffe, M. *Acta Crystallogr. A* **2007**, *63*, 418.

(14) Delgado-Friedrichs, O.; O'Keeffe, M.; Yaghi, O. M. *Phys. Chem. Chem. Phys.* **2007**, *9*, 1035.

(15) O'Keeffe, M.; Peskov, M. A.; Ramsden, S. J.; Yaghi, O. M. *Acc. Chem. Res.* **2008**, *41*, 1782. RCSR can be accessed at rcsr.anu.edu.au.

(16) (a) Ramsden, S. J.; Robins, V.; Hyde, S. T. *Acta Crystallogr. A* **2009**, *65*, 81. (b) Hyde, S. T.; Delgado-Friedrichs, O.; Ramsden, S. J.; Robins, V. *Solid State Sci.* **2006**, *8*, 740. EPINET can be accessed at epinet.anu.edu.au.

(17) (a) Blatov, V. A. *Cryst. Rev.* **2004**, *10*, 249. (b) Blatov, V. A. *IUCr CompComm Newsl.* **2006**, *7*, 4. TOPOS is available at www.topos.ssu.samara.ru.

(18) (a) Cubic: Fischer, W. *Acta Crystallogr. A* **2004**, *60*, 246. (b) Tetragonal: Fischer, W. *Acta Crystallogr. A* **2005**, *61*, 435. (c) Hexagonal: Sowa, H.; Koch, E. *Acta Crystallogr. A* **2006**, *62*, 379. (d) Orthorhombic: Sowa, H.; Fischer, W. *Acta Crystallogr. A* **2010**, *66*, 292. (e) Triclinic: Fischer, W.; Koch, E. *Acta Crystallogr. A* **2003**, *59*, 509. These papers give references to earlier work.

(19) Delgado-Friedrichs, O.; O'Keeffe, M. *J. Solid State Chem.* **2005**, *178*, 2480.

(20) The term "topology" is widely misused in many areas of chemistry, even to mean "structure", as noted: Francl, M. *Nature Chem.* **2009**, *1*, 334. We call attention to another misuse below.

(21) Delgado-Friedrichs, O.; O'Keeffe, M. *Acta Crystallogr. A* **2003**, *59*, 35. The program Systre is available at gavrog.org.

(22) O'Keeffe, M. *Zeits. Kristallogr.* **1991**, *196*, 21.

(23) Baerlocher, Ch.; McCusker, L. B.; Olson, D. H. *Atlas of Zeolite Framework Types*, 6th revised ed.; Elsevier: Amsterdam, 2007. www.iza-structure.org/databases/.

(24) Blatov, V. A.; O'Keeffe, M.; Proserpio, D. M. *CrystEngComm* **2010**, *12*, 44.

- (25) Blatov, V. A.; Delgado-Friedrichs, O.; O'Keeffe, M.; Proserpio, D. M. *Acta Crystallogr.* **2007**, *A63*, 418.
- (26) Alexandrov, E. V.; Blatov, V. A.; Kochetkov, A. V.; Proserpio, D. M. *CrystEngComm* **2011**, *12*, 3947.
- (27) Delgado-Friedrichs, O.; Foster, M. D.; O'Keeffe, M.; Proserpio, D. M.; Treacy, M. M. J.; Yaghi, O. M. *J. Solid State Chem.* **2005**, *178*, 2533.
- (28) Tranchemontagne, D. J.; Ni, Z.; O'Keeffe, M.; Yaghi, O. M. *Angew. Chem., Int. Ed.* **2008**, *47*, 5126.
- (29) Baburin, I. A.; Blatov, V. A. *Acta Crystallogr. B* **2007**, *63*, 79.
- (30) Vlasselaer, S.; D'Olieslager, W.; D'Hont, M. *J. Inorg. Nucl. Chem.* **1976**, *38*, 327.
- (31) Bennett, M. W.; Shores, M. P.; Beauvais, M. G.; Long, J. R. *J. Am. Chem. Soc.* **2000**, *122*, 6664.
- (32) Tranchemontagne, D. J.; Mendoza-Cortés, J. L.; O'Keeffe, M.; Yaghi, O. M. *Chem. Soc. Rev.* **2009**, *38*, 1257.
- (33) Li, H.; Eddaoudi, M.; Groy, T. J.; Yaghi, O. M. *J. Am. Chem. Soc.* **1998**, *120*, 8572.
- (34) (a) Chen, B.; Reineke, T. M.; Eddaoudi, M.; Kampf, J. W.; O'Keeffe, M.; Yaghi, O. M. *J. Am. Chem. Soc.* **2000**, *122*, 1559. (b) Kim, J.; Chen, B.; Reineke, T. M.; Li, H.; Eddaoudi, M.; Moler, D. B.; O'Keeffe, M.; Yaghi, O. M. *J. Am. Chem. Soc.* **2001**, *123*, 8239.
- (35) Wong-Foy, A. G.; Lebel, O.; Matzger, A. J. *J. Am. Chem. Soc.* **2007**, *129*, 15740.
- (36) Chun, H.; Kim, D.; Dybtsev, D. N.; Kim, K. *Angew. Chem., Int. Ed.* **2004**, *43*, 971.
- (37) Li, H.; Eddaoudi, M.; O'Keeffe, M.; Yaghi, O. M. *Nature* **1999**, *402*, 276.
- (38) Surble, S.; Serre, C.; Mellot-Draznieks, C.; Millange, F.; Férey, G. *Chem. Commun.* **2006**, 284.
- (39) (a) Ma, S.; Zhou, H.-C. *J. Am. Chem. Soc.* **2006**, *128*, 11734. (b) For a similar SBU, see also the following: Ma, S.; Wang, X.-S.; Yuan, D.; Zhou, H.-C. *Angew. Chem., Int. Ed.* **2008**, *47*, 130.
- (40) (a) Dinca, M.; Dailly, A.; Liu, Y.; Brown, C. M.; Neumann, D. A.; Long, J. R. *J. Am. Chem. Soc.* **2006**, *128*, 16874. (b) For a similar SBU, see also the following: Dinca, M.; Han, W. S.; Liu, Y.; Dailly, A.; Brown, C. M.; Long, J. R. *Angew. Chem., Int. Ed.* **2007**, *46*, 1419.
- (41) Cavka, J. H.; Jakobsen, S.; Olsbye, U.; Guillou, N.; Lamberti, C.; Bordiga, S.; Lillerud, K. P. *J. Am. Chem. Soc.* **2008**, *130*, 13850.
- (42) Chae, H. K.; Kim, J.; Delgado-Friedrichs, O.; O'Keeffe, M.; Yaghi, O. M. *Angew. Chem., Int. Ed.* **2003**, *42*, 3907.
- (43) (a) Chae, H. K.; Siberio-Pérez, D. Y.; Kim, J.; Go, Y.; Eddaoudi, M.; Matzger, A. J.; O'Keeffe, M.; Yaghi, O. M. *Nature* **2004**, *427*, 523. (b) Furukawa, H.; Ko, N.; Go, Y. B.; Aratani, N.; Choi, S. B.; Choi, E.; Yazaydin, A. Ö.; Snurr, R. Q.; O'Keeffe, M.; Kim, J.; Yaghi, O. M. *Science* **2010**, *329*, 424.
- (44) Natarajan, R.; Savitha, G.; Dominiak, P.; Wozniak, K.; Moorthy, J. N. *Angew. Chem., Int. Ed.* **2005**, *44*, 2115.
- (45) Sun, D.; Collins, D. J.; Ke, Y.; Zuo, J.-L.; Zhou, H. C. *Chem.—Eur. J.* **2006**, *12*, 3768.
- (46) Liu, Y.; Eubank, J. F.; Cairns, A. J.; Eckert, J.; Kravtsov, V. Ch.; Luebke, R.; Eddaoudi, M. *Angew. Chem., Int. Ed.* **2007**, *46*, 3278.
- (47) Chen, B.; Ockwig, N. W.; Millward, A. R.; Contreras, D. S.; Yaghi, O. M. *Angew. Chem., Int. Ed.* **2005**, *44*, 4745.
- (48) (a) Lin, X.; Jia, J.; Zhao, X.; Thomas, M.; Blake, A. J.; Walker, A. S.; Champness, N. R.; Hubberstey, P.; Schröder, M. *Angew. Chem., Int. Ed.* **2006**, *45*, 7358. (b) For other MOFs isoreticular with MOF-505, see: Hu, Y.; Xiang, S.; Zhang, W.; Zhang, Z.; Wang, L.; Bai, J.; Chen, B. *Chem. Commun.* **2009**, 7551.
- (49) Ma, L.; Falkowski, J. M.; Abney, C.; Lin, W. *Nat. Chem.* **2010**, *2*, 838.
- (50) Dahmam, T.; Rittner, P.; Böger-Siedel, S.; Gruehn, R. *J. Alloys Compd.* **1994**, *216*, 11.
- (51) (a) Iwamoto, T.; Shriver, D. F. *Inorg. Chem.* **1972**, *11*, 2570. (b) Abrahams, B. F.; Batten, S. R.; Hamit, H.; Hoskins, B. F.; Robson, R. *Angew. Chem., Int. Ed. Engl.* **1996**, *35*, 469. (c) Yuan, A.-H.; Ju, R.-Q.; Chen, Y.-Y.; Li, Y.-Z. *CrystEngComm.* **2010**, *12*, 1382.
- (52) Robl, G. *Mater. Res. Bull.* **1992**, *27*, 99.
- (53) Stein, O.; Ruschewitz, U. *Acta Crystallogr. E* **2005**, *61*, m2680.
- (54) Wang, F.-K.; Song, X.-K.; Yang, S.-Y.; Huang, R.-B.; Zheng, L.-S. *Inorg. Chem. Commun.* **2007**, *10*, 1198.
- (55) (a) Yang, S. Y.; Long, L. S.; Huang, R. B.; Zheng, L. S. *Chem. Commun.* **2002**, 472. (b) Yang, S. Y.; Long, L. S.; Jiang, Y. B.; Huang, R. B.; Zheng, L. S. *Chem. Mater.* **2002**, *14*, 3229.
- (56) Fang, Q.-R.; Zhu, G.-S.; Xue, M.; Zhang, Q.-L.; Sun, J.-Y.; Guo, X.-D.; Qiu, S.-L.; Xu, S.-T.; Wang, P.; Wang, D.-J.; Wei, Y. *Chem.—Eur. J.* **2006**, *12*, 3754.
- (57) Fang, Q.-R.; Zhu, G.-S.; Jin, Z.; Xue, M.; Wei, X.; Wang, D.-J.; Qiu, S.-L. *Angew. Chem., Int. Ed.* **2006**, *45*, 6126.
- (58) Sra, A. K.; Rombaut, G.; Lahitête, F.; Golhen, S.; Ouahab, L.; Mathonière, C.; Yakhmi, J. V.; Kahn, O. *New J. Chem.* **2000**, *24*, 871.
- (59) (a) Chun, H. *J. Am. Chem. Soc.* **2008**, *130*, 800. (b) Chun, H.; Jung, H.; Seo, J. *Inorg. Chem.* **2009**, *48*, 2043.
- (60) (a) Eddaoudi, M.; Kim, J.; Wachter, J. B.; Chae, H. K.; O'Keeffe, M.; Yaghi, O. M. *J. Am. Chem. Soc.* **2001**, *123*, 4368. (b) Moulton, B.; Lu, J.; Mondal, A.; Zaworotko, M. J. *Chem. Commun.* **2001**, 863.
- (61) Wang, H.-N.; Meng, X.; Yang, G.-S.; Wang, X.-L.; Shao, K. Z.; Su, Z.-M.; Wang, C.-G. *Chem. Commun.* **2011**, *47*, 7128.
- (62) (a) Nouar, F.; Eubank, J. F.; Bousquet, T.; Wojtas, L.; Zaworotko, M. J.; Eddaoudi, M. *J. Am. Chem. Soc.* **2008**, *130*, 1833. (b) Zhou, Y.; Park, M.; Hong, S.; Lah, M. S. *Chem. Commun.* **2008**, 2340.
- (63) (a) Hong, S.; Oh, M.; Park, M.; Yoom, J. W.; Chang, J.-S.; Lah, M. S. *Chem. Commun.* **2009**, 5397. (b) Zhao, D.; Yuan, D.; Sun, D.; Zhou, H.-C. *J. Am. Chem. Soc.* **2009**, *131*, 9186. (c) Yan, Y.; Telepeni, I.; Yang, S. H.; Lin, X.; Kockelmann, W.; Dailly, A.; Blake, A. J.; Lewis, W.; Walker, G. S.; Allan, D. R.; Barnett, S. A.; Champness, N. R.; Schroder, M. *J. Am. Chem. Soc.* **2010**, *132*, 4092. (d) Yuan, D.; Zhao, D.; Sun, D.; Zhou, H.-C. *Angew. Chem., Int. Ed.* **2010**, *49*, 5357.
- (64) Guo, Z.; Wu, H.; Srinivas, G.; Zhou, Y.; Xiang, S.; Chen, Z.; Yang, Y.; Zhou, W.; O'Keeffe, M.; Chen, B. *Angew. Chem., Int. Ed.* **2011**, *50*, 3178.
- (65) Moriera de Olivera, M.; Eon, J.-G. *Acta Crystallogr.* **2011**, *A67*, 240.
- (66) Chen, Z.; Xiang, S.; Liao, T.; Yang, Y.; Chen, S.; Zhou, Y.; Zhao, D.; Chen, B. *Cryst Growth Des.* **2010**, *10*, 2775.
- (67) Jia, J.; Sun, F.; Fang, Q.; Liang, X.; Cai, K.; Bian, Z.; Zhao, H.; Gao, L.; Zhu, G. *Chem. Commun.* **2011**, *47*, 9167.
- (68) Ma, L.; Mihalczik, D. J.; Lin, W. *J. Am. Chem. Soc.* **2009**, *131*, 4610.
- (69) Batten, S. R.; Hoskins, B. F.; Robson, R. *J. Am. Chem. Soc.* **1995**, *117*, 5385.
- (70) (a) Zhang, X.-M.; Zheng, Y.-Z.; Li, C.-R.; Zhang, W.-X.; Chen, X. M. *Cryst. Growth Des.* **2007**, *7*, 980. (b) Jia, J.; Lin, X.; Wilson, C.; Blake, A. J.; Champness, N. R.; Hubberstey, P.; Walker, G.; Cussen, E. J.; Schröder, M. *Chem. Commun.* **2007**, 840.
- (71) Volkringer, C.; Popov, D.; Loiseau, T.; Guillou, N.; Férey, G.; Haouas, M.; Taulelle, F.; Mellot-Draznieks, C.; Burghammer, M.; Riekkel, C. *Nature Mats.* **2007**, *6*, 760.
- (72) Zhang, X.-M.; Lv, J.; Ji, F.; Wu, H.-S.; Jiao, H.; Schleyer, P. v. R. *J. Am. Chem. Soc.* **2011**, *133*, 4788.
- (73) (a) Perry, J. J., IV; Kravtsov, V. Ch.; McManus, G. J.; Zaworotko, M. J. *J. Am. Chem. Soc.* **2007**, *129*, 10076. (b) Perry, J. J., IV; Perman, J. A.; Zaworotko, M. J. *Chem. Soc. Rev.* **2009**, *38*, 1400.
- (74) Wang, X.-S.; Ma, S.; Forster, P. M.; Yuan, D.; Eckert, J.; López, J. J.; Murphy, B. J.; Parise, J. B.; Zhou, H.-C. *Angew. Chem., Int. Ed.* **2008**, *47*, 7263.
- (75) Smaldone, R. A.; Forgon, R. S.; Furukawa, H.; Gassensmith, J. J.; Slawin, A. M. Z.; Yaghi, O. M.; Stoddart, J. F. *Angew. Chem., Int. Ed.* **2010**, *49*, 8630.
- (76) Férey, G.; Mellot-Draznieks, C.; Serre, C.; Millange, F.; Dutourm, J.; Surblé, S.; Margiolaki, I. *Science* **2005**, *239*, 2040.
- (77) O'Keeffe, M. *Mater. Res. Bull.* **2006**, *41*, 911.
- (78) Férey, G.; Serre, C.; Mellot-Draznieks, C.; Millange, F.; Surblé, S.; Dutour, J.; Margiolaki, I. *Angew. Chem., Int. Ed.* **2004**, *43*, 6296.
- (79) Park, Y. K.; Choi, S. B.; Kim, H.; Kim, K.; Won, B.-H.; Choi, K.; Choi, J.-S.; Ahn, W.-S.; Won, N.; Kim, S.; Jung, D. H.; Choi, S. H.; Kim,

- G.-H.; Cha, S.-S.; Jhon, Y. H.; Yang, J. K.; Kim, J. *Angew. Chem., Int. Ed.* **2007**, *46*, 8230.
- (80) Rosi, N. L.; Kim, J.; Eddaoudi, M.; Chen, B.; O'Keeffe, M.; Yaghi, O. M. *J. Am. Chem. Soc.* **2005**, *127*, 1504.
- (81) Férey, G.; Serre, C. *Chem. Soc. Rev.* **2009**, *38*, 109.
- (82) (a) Serre, C.; Millange, F.; Thouvenot, C.; Noguès, M.; Marsolier, G.; Louër, D.; Férey, G. *J. Am. Chem. Soc.* **2002**, *124*, 13519. (b) Barthelet, K.; Marrot, J.; Riou, D.; Férey, G. *Angew. Chem., Int. Ed.* **2002**, *41*, 28.
- (83) Rosi, N. L.; Eddaoudi, M.; Kim, J.; O'Keeffe, M.; Yaghi, O. M. *Angew. Chem., Int. Ed.* **2002**, *41*, 284.
- (84) Zhang, X.-H.; Hao, Z.-M.; Zhang, X.-M. *Chem.—Eur. J.* **2011**, *20*, 5585.
- (85) Colombo, V.; Galli, S.; Choi, H. J.; Han, G. D.; Maspero, A.; Palmisano, G.; Masciocchi, N.; Long, J. R. *Chem. Sci.* **2011**, *2*, 1311.
- (86) Bondar, O. A.; Lukashuk, L. V.; Lysenko, A. B.; Krautscheid, H.; Rusanov, E. B.; Chernega, A. N.; Domasevitch, K. V. *CrystEngComm* **2008**, *10*, 216.
- (87) (a) Perles, J.; Iglesias, M.; Martin-Liengo, M.-Á.; Monge, M. Á.; Valero, C.R.; Snejko, N. *Chem. Mater.* **2005**, *17*, 5837. (b) Miller, S. R.; Wright, P. A.; Serre, C.; Loiseau, T.; Marrot, J.; Férey, G. *Chem. Commun.* **2005**, 3850.
- (88) Monge, Á.; Gándara, F.; Gutiérrez-Pueblo, E.; Snejko, N. *CrystEngComm* **2011**, *13*, 5031.
- (89) (a) Gao, X. D.; Zhu, G. S.; Li, Z. Y.; Sun, F. X.; Yang, Z. H.; Qiu, S. L. *Chem. Commun.* **2006**, 3172. (b) Chen, B.; Yang, Y.; Zapata, F.; Lin, G.; Qian, G.; Lobkovsky, E. B. *Adv. Mater.* **2007**, *19*, 1693. (c) Gustavsson, M.; Bartosewicz, A.; Martin-Matute, N.; Sun, J.; Grins, J.; Zhao, T.; Li, Z.; Ahu, G.; Zou, X. *Chem. Mater.* **2011**, *22*, 3316.
- (90) Guo, Z.; Xu, H.; Su, S.; Cai, J.; Dang, S.; Xiang, S.; Qian, G.; Zhang, H.; O'Keeffe, M.; Chen, B. *Chem. Commun.* **2011**, *19*, 5551.
- (91) Gadipelli, S.; Ford, J.; Zhou, W.; Wu, H.; Udovic, T. J.; Yildirim, T. *Chem. Eur. J.* **2011**, *17*, 6043.
- (92) Dan-hardi, M.; Serre, C.; Frot, T.; Rozes, L.; Maurin, G.; Sanchez, C.; Férey, G. *J. Am. Chem. Soc.* **2011**, *131*, 10857.
- (93) Sumida, K.; Hill, M. R.; Horike, S.; Dailly, A.; Long, J. R. *J. Am. Chem. Soc.* **2009**, *131*, 15120.
- (94) Hyde, S. T.; Delgado-Friedrichs, O. *Solid State Sci.* **2011**, *13*, 676.